

# The distribution of galaxy rotation in JWST Advanced Deep Extragalactic Survey

Lior Shamir  

Kansas State University, Department of Computer Science, Manhattan, KS 66506, USA

Accepted 2025 February 12. Received 2025 February 12; in original form 2024 December 23

## ABSTRACT

JWST provides a view of the Universe never seen before, and specifically fine details of galaxies in deep space. JWST Advanced Deep Extragalactic Survey (JADES) is a deep field survey, providing unprecedentedly detailed view of galaxies in the early Universe. The field is also in relatively close proximity to the Galactic pole. Analysis of spiral galaxies by their direction of rotation in JADES shows that the number of galaxies in that field that rotate in the opposite direction relative to the Milky Way galaxy is  $\sim 50$  per cent higher than the number of galaxies that rotate in the same direction relative to the Milky Way. The analysis is done using a computer-aided quantitative method, but the difference is so extreme that it can be noticed and inspected even by the unaided human eye. These observations are in excellent agreement with deep fields taken at around the same footprint by *Hubble Space Telescope* and JWST. The reason for the difference may be related to the structure of the early Universe, but it can also be related to the physics of galaxy rotation and the internal structure of galaxies. In that case the observation can provide possible explanations to other puzzling anomalies such as the  $H_0$  tension and the observation of massive mature galaxies at very high redshifts.

**Key words:** galaxies: general – galaxies: spiral – early Universe – large-scale structure of Universe.

## 1 INTRODUCTION

JWST has introduced unprecedented imaging power, allowing it to capture high visual details of astronomical objects in deep space. The ability to identify shapes of objects in the very early Universe has a transformative impact on astronomy and cosmology. An example is the galaxies identified at very high redshifts (Adams et al. 2023; Boylan-Kolchin 2023; Bradley et al. 2023; Carniani et al. 2024), such as JADES-GS-z14-0 at redshift of  $\sim 14.2$ , and just  $\sim 0.25$  Gyr after the big bang (Carniani et al. 2024; Helton et al. 2024; Jones et al. 2025; Schouws et al. 2024). Galaxies at unexpectedly high redshift also include Milky Way-like spiral galaxies (Costantin et al. 2023; Jain & Wadadekar 2024), showing that such galaxies are also present at relatively high-redshift ranges (Kuhn et al. 2024). Although spiral galaxies at unexpectedly high redshifts were known before JWST was launched (Tsukui & Iguchi 2021), the visual observations enabled by JWST are considered surprising given the current cosmological and galaxy formation theories (Adil et al. 2023; Boylan-Kolchin 2023; Forconi et al. 2023; Gupta 2023; Melia 2023; Xiao et al. 2024).

Additionally, the yet unexplained  $H_0$  tension (Wu & Huterer 2017; Bolejko 2018; Mörtsell & Dhawan 2018; Davis et al. 2019; Camarena & Marra 2020; Pandey, Raveri & Jain 2020; Di Valentino et al. 2021; Riess et al. 2022) introduces a substantial challenge to cosmology, and it has been suggested that the  $H_0$  tension and high-redshift galaxies observed by JWST are linked (Shen et al. 2024).

While research is bound to continue, the unexpected observations made so far by JWST have been argued to be in tension with standard cosmology (Dolgov 2023; Forconi et al. 2023; Gupta 2023, 2024a, b; Lovell et al. 2023; Wang & Liu 2023; Muñoz et al. 2024).

One of the observations enabled by the ability of JWST to identify high visual details of galaxies is the alignment between the galaxy direction of rotation as observed by JWST and the direction of rotation of the Milky Way (Shamir 2024e). Namely, JWST shows a much higher number of galaxies that rotate in the opposite direction relative to the Milky Way. That can be observed in JWST deep fields taken at close proximity to the Galactic pole. When spiral galaxies are located at around the Galactic pole, their direction of rotation can determine whether they rotate in the same direction relative to the Milky Way, or in the opposite direction relative to the Milky Way (Shamir 2024e).

A first observation of the higher prevalence of galaxies that rotate in opposite direction relative to the Milky Way in JWST deep fields was reported in Shamir (2024e). The analysis was based on a preliminary JWST deep field image taken inside the field of the *Hubble Space Telescope* (*HST*) Ultra Deep Field (UDF). The deep field was imaged in 2022 October, and the image was released to the public on 2023 April. Analysis of the field (Shamir 2024e) identified 33 galaxies with identifiable direction of rotation, where 23 of them rotated in the opposite direction relative to the Milky Way ( $p \simeq 0.012$ ). Fig. 1 shows the deep field annotated by the direction of rotation of the galaxies (Shamir 2024e).

When done manually, the determination of the direction of rotation of a galaxy can be a subjective task, as different annotators might have different opinions regarding the direction towards a galaxy

\* E-mail: [lshamir@mtu.edu](mailto:lshamir@mtu.edu)

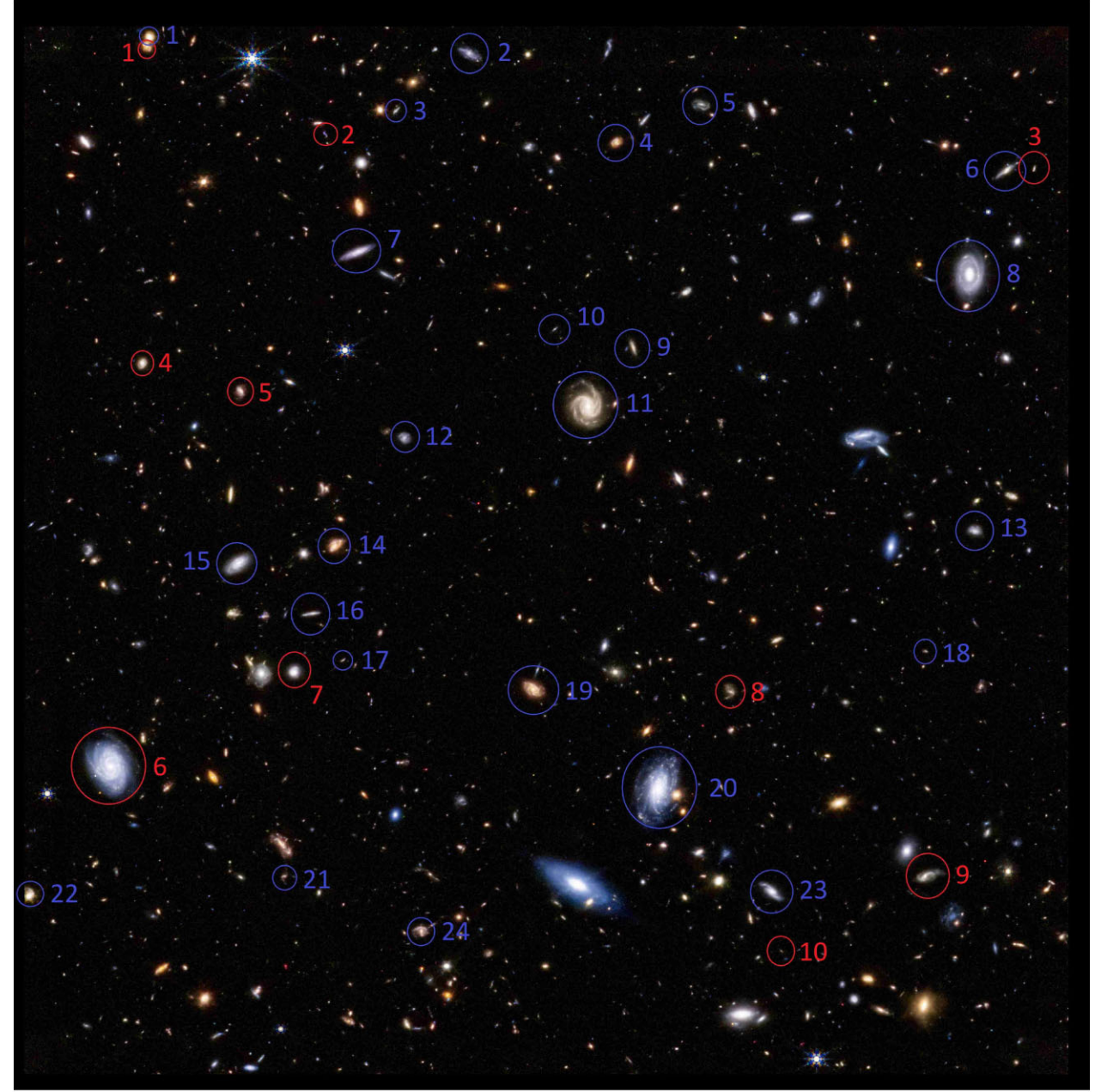


**Figure 1.** Spiral galaxies imaged by *JWST* that rotate in the same direction relative to the Milky Way (red) and in the opposite direction relative to the Milky Way (blue). The number of galaxies rotating in the opposite direction relative to the Milky Way as observed from Earth is far higher (Shamir 2024e).

rotates. A simple example is the crowdsourcing annotation through Galaxy Zoo 1 (Land et al. 2008), where in the vast majority of the galaxies different annotators provided conflicting annotations. Therefore, the annotations shown in Fig. 1 were made by a computer analysis that followed a defined symmetric model (Shamir 2024e). Yet, the advantage of the analysis of the relatively small *JWST* deep field is that it can be inspected by the human eye to ensure that the annotations of the galaxies are consistent, and that no population of non-annotated galaxies that could change the outcome of the analysis exists (Shamir 2024e).

The difference between the number of galaxies that rotate in opposite directions was also noticed when using Earth-based telescopes (MacGillivray & Dodd 1985; Longo 2011; Shamir 2012, 2016, 2019, 2020b, c, d, 2021a, b, 2022a, b, d, e). Namely, it has been shown that

the difference between the number of galaxies that rotate in opposite directions increases as the redshift gets higher (Shamir 2019, 2020d, 2022d, 2024d), which might suggest that the difference becomes larger in the deep Universe as imaged by *JWST*. On the other hand, several studies argued that the distribution is random (Iye & Sugai 1991; Land et al. 2008; Hayes, Davis & Silva 2017; Tadaki et al. 2020; Iye, Yagi & Fukumoto 2021; Patel & Desmond 2024). These studies will be discussed in Section 4 of this paper. But with the imaging power of *JWST*, the uneven distribution becomes clear, and can be verified even with the unaided human eye (Shamir 2024e). This paper analyses the distribution of spiral galaxies in the JADES survey. Any anomaly in the distribution can be related to the structure of the early universe, but can also be driven by the mysterious physics of galaxy rotation.

While several analyses using different instruments were performed, *JWST* introduces new opportunities to study the asymmetry in the early Universe. The imaging power of *JWST* is particularly meaningful because the magnitude of the asymmetry has been identified to grow as the redshift gets larger (Shamir 2019, 2020d, 2022d, 2024d), and therefore studying the asymmetry in deep fields can lead to new observations. This paper examines the possibility of an anomaly in the distribution of galaxies rotating in opposite directions in the *JWST* deep fields as observed from Earth. The observation is compared to analyses with other space- and Earth-based telescopes that image the same field, as well as other parts of the entire sky.

## 2 DATA

The data used in this analysis is taken from the GOODS-S field of *JWST* Advanced Deep Extragalactic Survey (JADES). JADES (Eisenstein et al. 2023; Bunker et al. 2024) is the largest deep field imaging program planned for the early operation of *JWST*, focusing on the well-studied Great Observatories Origins Deep Survey South (GOODS-S) and Great Observatories Origins Deep Survey North (GOODS-N) fields. The image data are acquired primarily through the near-infrared camera (NIRCam).

The image data used for the analysis was based on the *JWST* 4.4, 2.0, and 0.9  $\mu\text{m}$  bands visualized through the red giant branch channels, providing an informative form of visualization that allows for effective analysis. Parts of the JADES GOODS-S field that did not have these three channels were not used in the analysis. The RA of the objects used in this study ranged from  $53.01885^\circ$  to  $53.2184^\circ$ , and the declination ranged between  $-27.9145^\circ$  to  $-27.7292^\circ$ .

The galaxies were annotated by their direction of rotation as done in Shamir (2024e). The analysis was automatic, and followed a defined model that allows to define the direction of rotation of a galaxy in an objective and consistent manner. As also briefly mentioned in Introduction, manual annotation of the direction of rotation of a galaxy can be subjective, and different people might have different opinions when they need to determine the direction of rotation of a galaxy. It has also been shown that such annotation can be driven by consistent biases, so even a group of people annotating the same galaxy cannot provide consistent annotations in all cases (Land et al. 2008). For that reason, while manual annotation should be used to verify the consistency of the annotation, it cannot be considered a sound scientific methodology that such annotation can rely on.

Deep convolutional neural networks (CNNs) have become the most common solution to tasks related to image classification tasks. Their popularity is driven by excellent performance, as well as the availability of easy-to-use libraries that make the analysis accessible also to researchers who do not necessarily have strong computing skills. The primary downside of CNNs is that they are driven by highly complex data-driven rules that are very difficult to understand. Therefore, they are subjected to biases that can be highly difficult to identify (Dhar & Shamir 2021; Ball 2023; Erkude, Joshi & Shamir 2024). Such biases can be driven by the manual selection of training samples, as two neural networks trained with two different training sets will also perform differently. In the case of astronomical images, even the distribution of the training galaxy images in the sky can lead to different results (Dhar & Shamir 2022). Therefore, using CNNs for the annotation of the galaxies cannot be considered a sound solution when the analysis needs to be clear, and certain conditions such as the symmetry of the algorithm need to be guaranteed.



**Figure 2.** Example of the same galaxies imaged by DES (left) and by *JWST*. *JWST* allows to analyse galaxies that DES or other Earth-based telescopes cannot image with sufficient details to identify their direction of rotation.

Clearly, the annotation of the galaxies is not complete, as some of the galaxies are not assigned with a direction of rotation, and are therefore excluded from the analysis. Some of the galaxies may be elliptical, and other galaxies may not have clear visual details that are sufficient to identify their direction of rotation. Fig. 2 shows examples of galaxies imaged by both Dark Energy Survey (DES) and *JWST*. While the DES images do not provide sufficient visual details, the *JWST* images allow to identify the direction of rotation of the galaxies. Therefore, *JWST* can provide an analysis of the direction of rotation of galaxies that cannot be imaged by DES or by any other existing Earth-based telescope.

The annotations were done by using the Ganalyzer algorithm (Shamir 2011a, b) and also used in Shamir (2011b, 2013, 2016, 2017a, b, c, 2020b, c, 2021a, b, 2022b, d, e, 2024e). The algorithm is based on a first step of separating foreground objects from the background. After each object is separated from the image, it is transformed into its radial intensity plot transformation.

The radial intensity plot captures the object intensity variations at different distances from its centre. It is a  $35 \times 360$  matrix, where the intensity of the pixel  $(x, y)$  is the median intensity of the  $5 \times 5$  pixels centred at  $(O_x + \sin(\theta) \cdot r, O_y - \cos(\theta) \cdot r)$  in the original image, where  $r$  is the radial distance from the centre  $(O_x, O_y)$ , and  $\theta$  is the polar angle (Shamir 2011b).

Because the arms of a galaxy are brighter than the non-arm part of the galaxy at the same distance from the galaxy centre, the arm pixels can be identified by a peak detection algorithm (Morpháč et al. 2000) applied to each line in the radial intensity plot. Applying a linear regression to the peaks provides the slope of the line formed by them, and the sign of the slope determines the direction towards which the arm of the galaxy is curved. To avoid elliptical galaxies or galaxies that do not have a clear direction of rotation, galaxies that have less than 30 peaks are considered galaxies that do not have an identifiable direction of rotation. Also, the slope of the linear regression needs to be at least 0.35 (Shamir 2011b), otherwise the galaxy is not assigned with a direction of rotation, and therefore is not used in the analysis. Fig. 3 shows examples of galaxies as imaged by *JWST* as used in this study, and their radial intensity plots that allow to identify their direction of rotation. The process is described with empirical analysis and experimental results in Shamir (2011b,

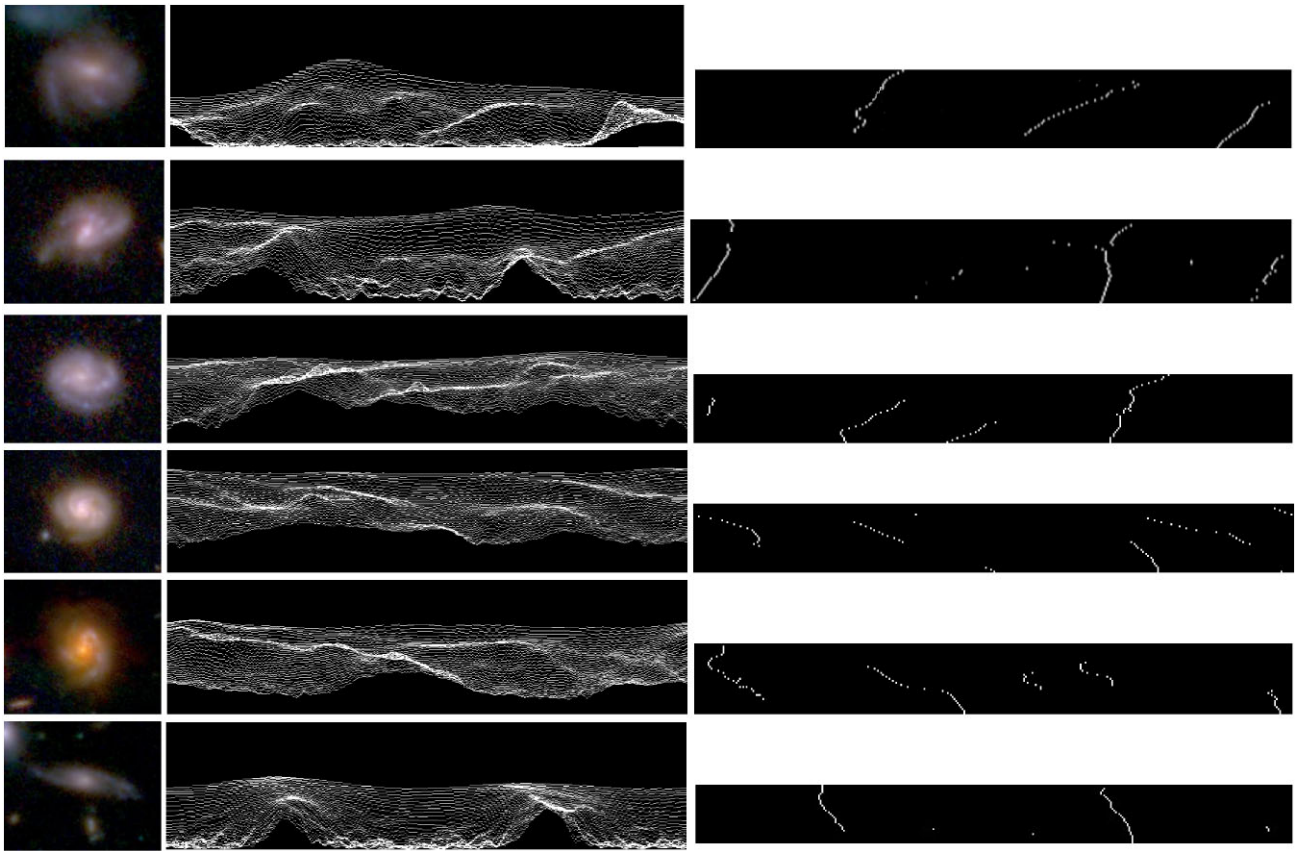


**Figure 3.** Example of galaxies imaged by *JWST* and the peaks of the radial intensity plot transformations of each image. The lines formed by the peaks allow to identify the direction of the curve of the arms, and consequently the spin direction of the galaxy.

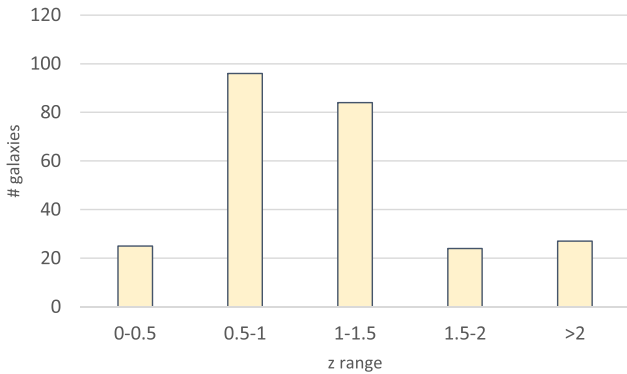


**Figure 4.** The redshift distribution of the *JWST* galaxies used in the study.

2013, 2016, 2017a, b, c, 2020b, c, 2021a, b, 2022b, d, e). Namely, it has been used to analyse initial *JWST* deep field images taken inside the footprint of GOODS-S (Shamir 2024e).

The process led to 263 galaxies with identified direction of rotation. Fig. 4 shows the distribution of the redshift of the galaxies.

While the algorithm is defined and symmetric, to ensure the symmetric nature of the analysis the entire field was mirrored, and the algorithm was applied to the mirrored image. Results were exactly inverse, which can be expected since the algorithm is symmetric, and was tested in a similar manner in previous experiments (Shamir 2011b, 2013, 2016, 2017a, b, c, 2020b, c, 2021a, b, 2022b, d, e, 2024e).

The annotation algorithm determines the directions of rotation of the galaxies by the curves of the arms. The arms of spiral galaxies have been shown to be a very reliable probe for determining the direction of rotation of the stellar mass as it rotates around the galaxy centre. For instance, De Vaucouleurs (1958) used the galaxy spectra and dust silhouette to study the link between the direction of rotation and shape of the galaxy arms, and found that in all cases the spiral arms were trailing. A more recent study (Iye, Tadaki & Fukumoto 2019) also found that all galaxies that were examined have trailing arms, and therefore the shape of the arm is a strong indication of the direction of rotation of the stellar mass. In some very rare cases galaxies can also have leading arms. A known example of a galaxy with leading arms is NGC 4622 (Freeman, Byrd & Howard 1991; Byrd & Howard 2019), but these cases are extremely rare.

### 3 RESULTS

The application of the image processing to the *JWST* GOODS-S image data as described in Section 2 provided annotations for 263 galaxies that their direction of rotation was identified. Of these galaxies, 105 rotate counterclockwise, while 158 rotate clockwise. Assuming that the probability of a galaxy to rotate in a certain direction is completely random, the one-tailed binomial distribution probability to have such asymmetry or stronger by chance is  $\sim 0.0007$ , which is  $\sim 3.39\sigma$ .

Figs 5 and 6 show the galaxies in the field that were identified as rotating in the same direction relative to the Milky Way (counterclockwise) and the galaxies that rotate in the opposite direction

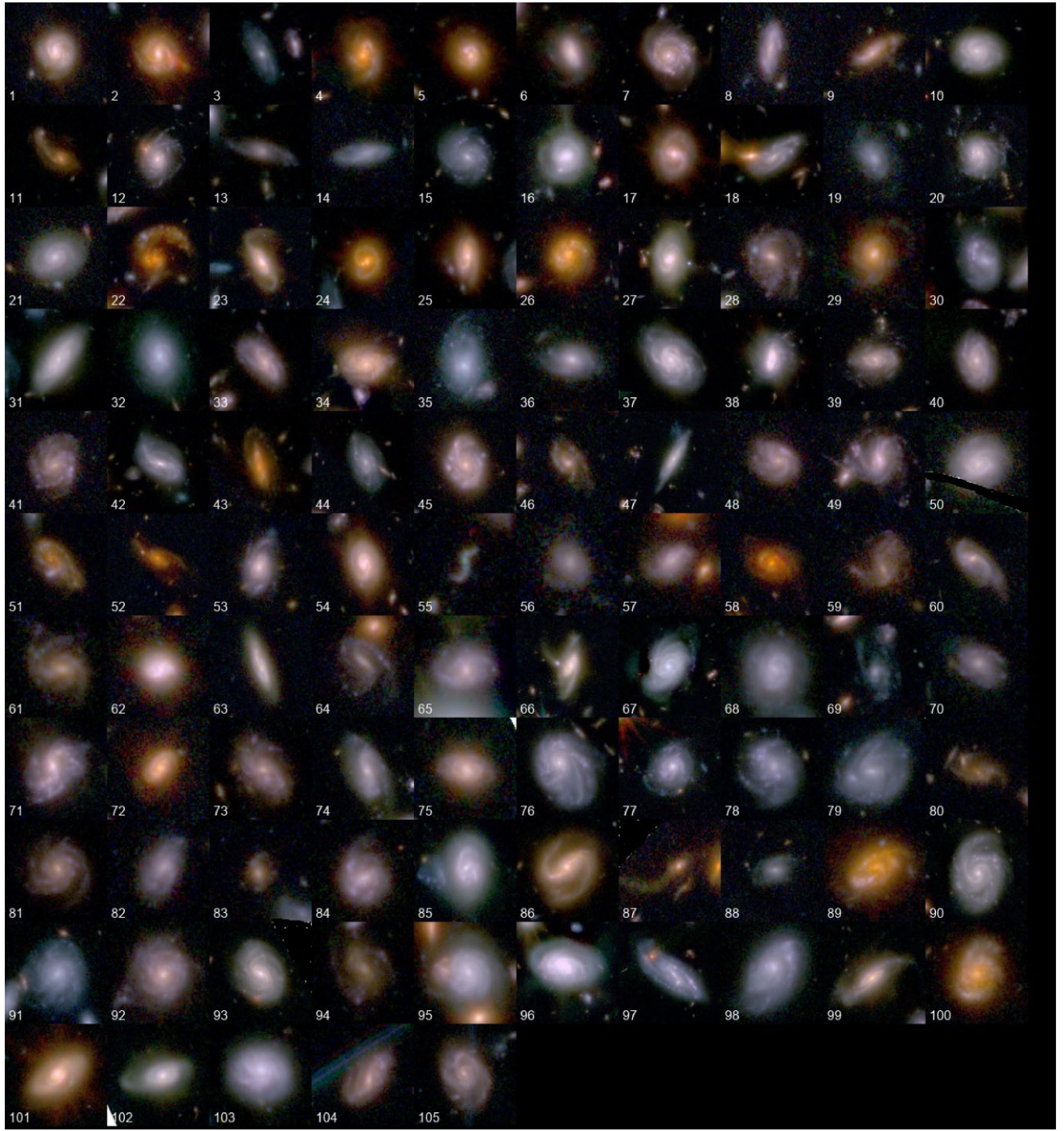


**Figure 5.** The galaxies in the JADES GOODS-S field that were identified as rotating in the same direction relative to the Milky Way (counterclockwise). The  $(\alpha, \delta)$  coordinates of each galaxy are specified in Table 1.

relative to the Milky Way (clockwise), respectively. Tables 1 and 2 provide the coordinates of each of the 263 galaxies. Fig. 7 shows the location of the galaxies inside the JADES GOODS-S field. While the unaided human eye might not be a fully sound tool to annotate the galaxies, visual inspection shows consistency between the annotation of the algorithm and the human eye, and no galaxy seems to be identified incorrectly.

Visual inspection of the galaxies that were identified shows no galaxy that was annotated incorrectly. But the annotation algorithm

also avoids annotating galaxies that their direction of rotation cannot be identified. These may be elliptical galaxies, or galaxies that the visual details of their arms do not allow the identification of their direction of rotation. Because the algorithm is symmetric, galaxies that their direction of rotation could not be identified by the algorithm are expected to be treated in the same manner regardless of their direction of rotation. Still, it is important to also inspect the population of galaxies that the algorithm could not identify their direction of rotation.

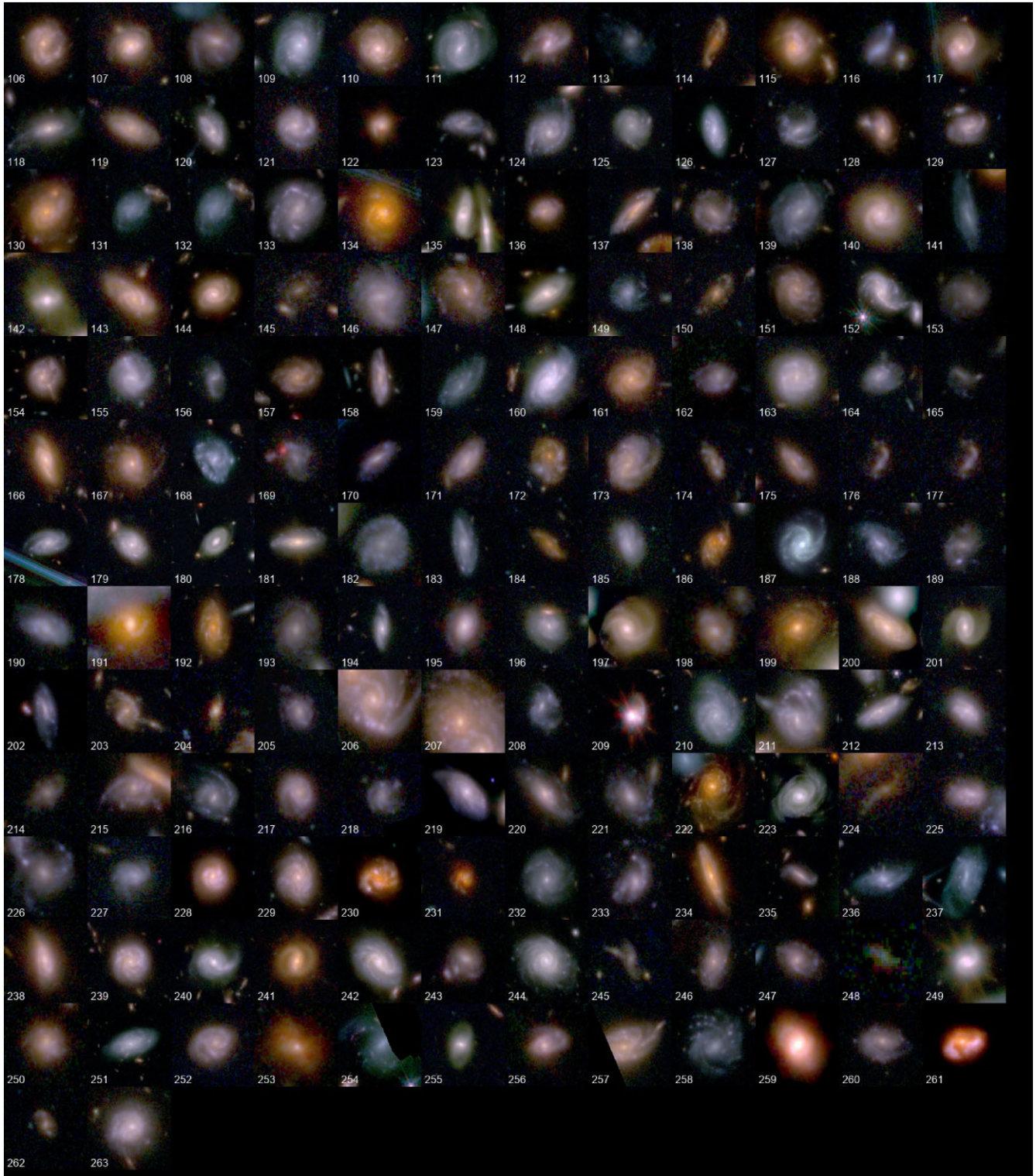


**Figure 6.** The galaxies in the JADES GOODS-S field that were identified as rotating in the opposite direction relative to the Milky Way. The coordinates of each galaxy are specified in Table 2.

As was done in Shamir (2024e), the field was inspected manually to identify galaxies that their direction of rotation was not identified by the algorithm. Figs 8 and 9 show galaxies that perhaps could be considered as rotating counterclockwise and clockwise, respectively.

The rotation of direction is not entirely clear in these images, but these galaxies were the most clear galaxies among those galaxies that were not identified by the algorithm. As mentioned before, manual observation is not a sound scientific manner to identify the

**Table 1.** The RA and Dec. of the galaxies that rotate counterclockwise shown in Fig. 5.

| Numbers | RA         | Dec.        | Numbers | RA         | Dec.        | Numbers | RA         | Dec.        |
|---------|------------|-------------|---------|------------|-------------|---------|------------|-------------|
| 1       | 53.0287575 | -27.8703469 | 2       | 53.0305730 | -27.8557305 | 3       | 53.0346279 | -27.8713092 |
| 4       | 53.0367451 | -27.8875751 | 5       | 53.0373338 | -27.8703302 | 6       | 53.0425003 | -27.8821344 |
| 7       | 53.0442441 | -27.8953532 | 8       | 53.0460538 | -27.8289356 | 9       | 53.0467626 | -27.8520855 |
| 10      | 53.0495568 | -27.8992607 | 11      | 53.0508248 | -27.8919429 | 12      | 53.0514024 | -27.8701501 |
| 13      | 53.0552519 | -27.8856482 | 14      | 53.0558147 | -27.8300434 | 15      | 53.0567343 | -27.8796932 |
| 16      | 53.0578412 | -27.8307351 | 17      | 53.0585653 | -27.8568762 | 18      | 53.0605633 | -27.8512857 |
| 19      | 53.0606090 | -27.8310224 | 20      | 53.0625037 | -27.8349052 | 21      | 53.0629972 | -27.8310975 |
| 22      | 53.0689231 | -27.8796888 | 23      | 53.0704161 | -27.9052013 | 24      | 53.0717760 | -27.8437142 |
| 25      | 53.0720162 | -27.8537413 | 26      | 53.0727344 | -27.8343114 | 27      | 53.0752012 | -27.8314599 |
| 28      | 53.0772016 | -27.8205387 | 29      | 53.0778957 | -27.8932042 | 30      | 53.0781977 | -27.8701926 |
| 31      | 53.0782543 | -27.8569828 | 32      | 53.0794105 | -27.8623380 | 33      | 53.0796836 | -27.8424121 |
| 34      | 53.0803383 | -27.9005456 | 35      | 53.0803688 | -27.8083994 | 36      | 53.0810023 | -27.8238445 |
| 37      | 53.0819773 | -27.8399439 | 38      | 53.0844410 | -27.8728831 | 39      | 53.0878515 | -27.8308227 |
| 40      | 53.0951927 | -27.8568509 | 41      | 53.0956144 | -27.8159647 | 42      | 53.1018111 | -27.8650500 |
| 43      | 53.1031616 | -27.8652455 | 44      | 53.1074863 | -27.8623169 | 45      | 53.1077205 | -27.8388817 |
| 46      | 53.1081399 | -27.8877607 | 47      | 53.1083292 | -27.8795013 | 48      | 53.1085802 | -27.8633293 |
| 49      | 53.1103699 | -27.8883061 | 50      | 53.1107677 | -27.8339117 | 51      | 53.1108220 | -27.8006488 |
| 52      | 53.1131144 | -27.8866044 | 53      | 53.1155528 | -27.9144036 | 54      | 53.1155789 | -27.8447307 |
| 55      | 53.1187014 | -27.8057706 | 56      | 53.1237878 | -27.8326410 | 57      | 53.1239903 | -27.8631171 |
| 58      | 53.1245910 | -27.8932989 | 59      | 53.1262410 | -27.8292075 | 60      | 53.1272777 | -27.8386627 |
| 61      | 53.1301701 | -27.7809458 | 62      | 53.1326939 | -27.8329912 | 63      | 53.1338997 | -27.8516127 |
| 64      | 53.1352184 | -27.8750690 | 65      | 53.1373614 | -27.7622325 | 66      | 53.1374871 | -27.8418249 |
| 67      | 53.1437771 | -27.8134799 | 68      | 53.1454738 | -27.7506179 | 69      | 53.1454750 | -27.8336683 |
| 70      | 53.1462674 | -27.8314869 | 71      | 53.1499913 | -27.7399957 | 72      | 53.1507510 | -27.8574200 |
| 73      | 53.1508711 | -27.7419219 | 74      | 53.1523853 | -27.8343908 | 75      | 53.1554348 | -27.7661381 |
| 76      | 53.1564312 | -27.8108991 | 77      | 53.1564439 | -27.8710278 | 78      | 53.1581806 | -27.7811417 |
| 79      | 53.1589977 | -27.8326493 | 80      | 53.1595345 | -27.8392275 | 81      | 53.1598219 | -27.7623367 |
| 82      | 53.1600056 | -27.7669025 | 83      | 53.1603471 | -27.8406146 | 84      | 53.1618000 | -27.7292176 |
| 85      | 53.1624406 | -27.7751180 | 86      | 53.1635603 | -27.7589436 | 87      | 53.1637381 | -27.8514252 |
| 88      | 53.1643375 | -27.8658913 | 89      | 53.1675906 | -27.8304041 | 90      | 53.1698898 | -27.7710453 |
| 91      | 53.1726089 | -27.7964452 | 92      | 53.1754466 | -27.7496166 | 93      | 53.1801809 | -27.7989112 |
| 94      | 53.1852851 | -27.7685314 | 95      | 53.1862976 | -27.8230718 | 96      | 53.1868309 | -27.7910178 |
| 97      | 53.1879238 | -27.7940122 | 98      | 53.1902891 | -27.7401635 | 99      | 53.1951860 | -27.7538285 |
| 100     | 53.2015172 | -27.7472044 | 101     | 53.2023884 | -27.7513782 | 102     | 53.2046668 | -27.7553699 |
| 103     | 53.2064105 | -27.7750928 | 104     | 53.2131711 | -27.7718123 | 105     | 53.2181259 | -27.7658299 |

direction of rotation of the galaxies due to its subjective nature. These galaxies were not used in the analysis, but just to inspect the kind of galaxies that were not annotated by the algorithm. The manual inspection does not show a certain pattern of galaxies that their direction of rotation was not identified by the algorithm. The coordinates of the galaxies in both figures are specified in Tables 3 and 4.

*JWST* provides visual details of galaxies in the deep Universe, and far deeper than any other telescope. But the unequal number of galaxies that rotate in opposite directions around the Galactic poles was noticed also with Earth-based telescopes, although the differences were smaller than the difference observed in the deeper Universe using *JWST*. For instance, Fig. 10 shows the difference between the number of galaxies with opposite directions of rotation in different parts of the sky, as determined by using a large dataset of  $1.3 \times 10^6$  galaxies annotated by their direction of rotation (Shamir 2022e). The galaxy images were collected by the Dark Energy Spectroscopic Instrument (DESI) Legacy Survey, and the analysis was done before *JWST* was launched. The difference between galaxies that rotate in opposite directions in the different parts of the sky are quantified by  $\frac{cw-cw}{cw+ccw}$  in the hemisphere centred at each integer ( $\alpha, \delta$ ) combination, and displayed by the colour such that red parts of the sky indicate a higher number of galaxies rotating clockwise, and blue parts of the sky reflect a higher number of galaxies rotating counterclockwise.

The figure shows simple direct measurements of the differences in different parts of the sky, and not an attempt to fit the distribution to a certain pre-determined model. The image and the analysis through which it was generated are explained in full detail in Shamir (2022e).

The figure shows a higher asymmetry in both ends of the Galactic poles, where in both end there is a higher number of galaxies that rotate in the opposite directions relative to the Milky Way galaxy. GOODS-S is located in relatively close proximity to the Southern Galactic pole, and therefore the difference can be expected based on previous observations made before *JWST* was launched. Previous observations using Earth-based telescopes also showed that the magnitude of the asymmetry increases as the redshift gets higher (Shamir 2020d). If that trend continues into the higher redshift ranges, it can also explain the higher asymmetry in the much higher redshift of the galaxies imaged by *JWST*.

‘Webb’s First Deep Field’ was also tested in the same manner, providing no statistically significant asymmetry with 21 galaxies rotating counterclockwise, and 19 galaxies that rotate clockwise (Shamir 2024e). That field is not close to neither ends of the Galactic pole, so asymmetry is not expected in that field based on the analysis done with DESI Legacy Survey (Shamir 2022e) before *JWST* was launched.

**Table 2.** The RA and Dec. of the galaxies that rotate clockwise shown in Fig. 6.

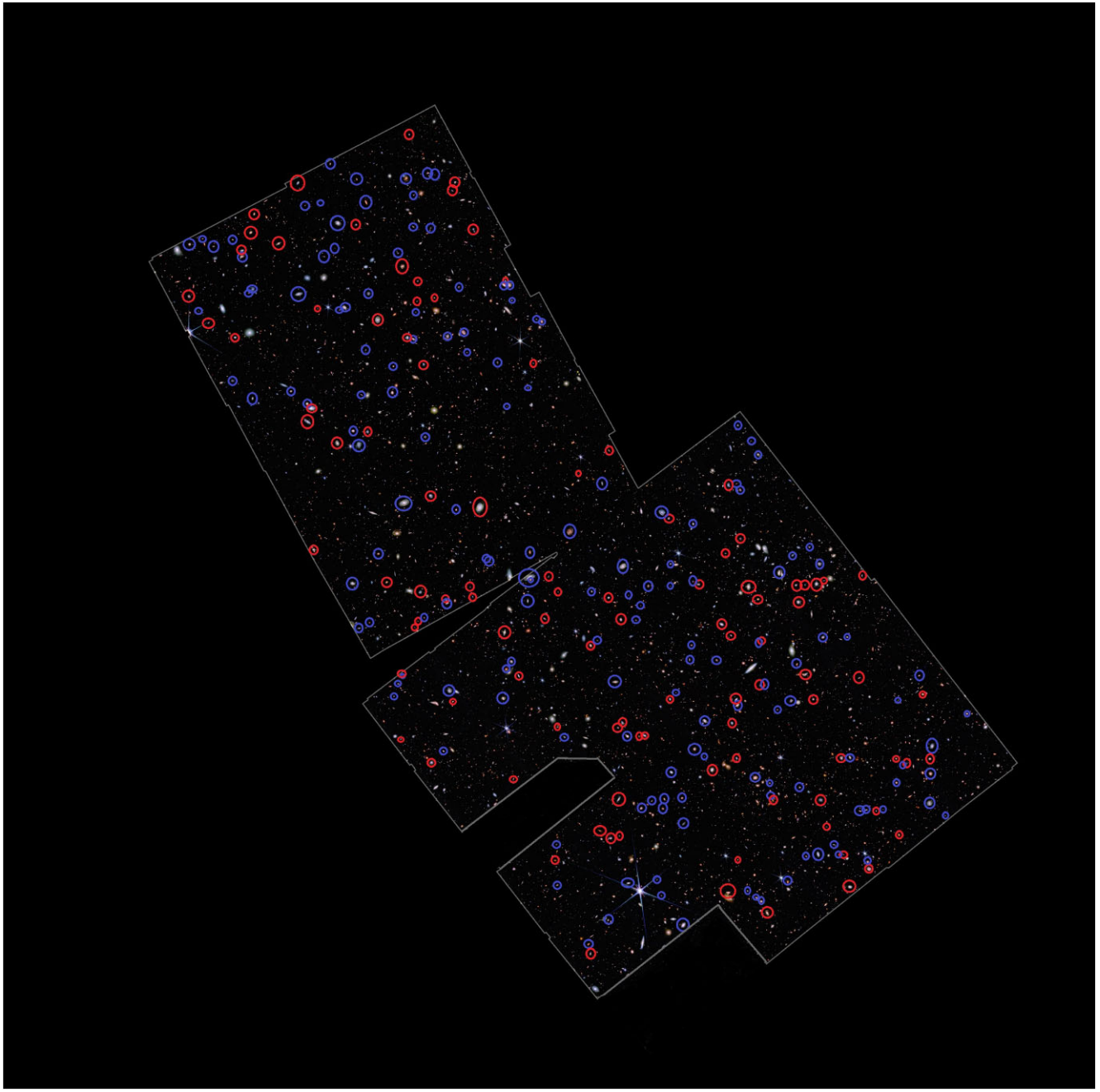
| Numbers | RA         | Dec.        | Numbers | RA         | Dec.        | Numbers | RA         | Dec.        |
|---------|------------|-------------|---------|------------|-------------|---------|------------|-------------|
| 106     | 3.1279542  | -27.7715134 | 107     | 53.0193353 | -27.8602004 | 108     | 53.0248564 | -27.8832216 |
| 109     | 53.0281374 | -27.8675260 | 110     | 53.0286673 | -27.8737467 | 111     | 53.0289134 | -27.8803077 |
| 112     | 53.0315505 | -27.8515717 | 113     | 53.0357380 | -27.8716810 | 114     | 53.0368943 | -27.8572009 |
| 115     | 53.0373588 | -27.8758075 | 116     | 53.0408007 | -27.8817782 | 117     | 53.0446664 | -27.8936859 |
| 118     | 53.0450450 | -27.8818705 | 119     | 53.0465296 | -27.8821387 | 120     | 53.0492605 | -27.8700264 |
| 121     | 53.0499228 | -27.8428186 | 122     | 53.0521408 | -27.8920364 | 123     | 53.0533498 | -27.8897312 |
| 124     | 53.0561208 | -27.8427935 | 125     | 53.0569792 | -27.8262655 | 126     | 53.0573808 | -27.8919577 |
| 127     | 53.0595572 | -27.8224721 | 128     | 53.0604167 | -27.8924328 | 129     | 53.0620101 | -27.8768390 |
| 130     | 53.0627890 | -27.8489887 | 131     | 53.0638817 | -27.8243501 | 132     | 53.0639208 | -27.8243688 |
| 133     | 53.0642316 | -27.8572046 | 134     | 53.0650035 | -27.8981819 | 135     | 53.0673265 | -27.8282897 |
| 136     | 53.0678622 | -27.8592175 | 137     | 53.0693205 | -27.8788218 | 138     | 53.0697243 | -27.8758420 |
| 139     | 53.0710796 | -27.8537283 | 140     | 53.0717995 | -27.9025473 | 141     | 53.0722817 | -27.8443486 |
| 142     | 53.0727420 | -27.8012799 | 143     | 53.0731238 | -27.9018674 | 144     | 53.0734710 | -27.8746265 |
| 145     | 53.0745397 | -27.7985159 | 146     | 53.0753324 | -27.9002020 | 147     | 53.0772981 | -27.8095869 |
| 148     | 53.0779581 | -27.8582796 | 149     | 53.0780646 | -27.7948371 | 150     | 53.0782010 | -27.8081526 |
| 151     | 53.0832777 | -27.8480718 | 152     | 53.0862719 | -27.8617956 | 153     | 53.0864800 | -27.8698430 |
| 154     | 53.0888870 | -27.8681537 | 155     | 53.0893112 | -27.8172391 | 156     | 53.0893392 | -27.8302602 |
| 157     | 53.0897244 | -27.8446916 | 158     | 53.0902375 | -27.8479062 | 159     | 53.0917752 | -27.8850705 |
| 160     | 53.0917947 | -27.9079949 | 161     | 53.0921738 | -27.8791953 | 162     | 53.0937000 | -27.8554013 |
| 163     | 53.0942337 | -27.8755992 | 164     | 53.0951142 | -27.8262703 | 165     | 53.0951248 | -27.8313279 |
| 166     | 53.0966713 | -27.8793750 | 167     | 53.0970239 | -27.8816290 | 168     | 53.0971496 | -27.8146692 |
| 169     | 53.0973401 | -27.9013593 | 170     | 53.0985649 | -27.8976944 | 171     | 53.0998786 | -27.8798943 |
| 172     | 53.1007743 | -27.8312572 | 173     | 53.1025891 | -27.8815702 | 174     | 53.1027136 | -27.8357093 |
| 175     | 53.1039113 | -27.8390226 | 176     | 53.1058087 | -27.8334029 | 177     | 53.1058206 | -27.8334083 |
| 178     | 53.1058432 | -27.8984435 | 179     | 53.1060740 | -27.8652313 | 180     | 53.1073507 | -27.8267313 |
| 181     | 53.1091200 | -27.8530365 | 182     | 53.1109910 | -27.9067594 | 183     | 53.1125336 | -27.8080579 |
| 184     | 53.1137720 | -27.8435787 | 185     | 53.1152094 | -27.8325756 | 186     | 53.1160406 | -27.9121885 |
| 187     | 53.1207774 | -27.8189708 | 188     | 53.1221556 | -27.8654683 | 189     | 53.1242332 | -27.8897040 |
| 190     | 53.1293315 | -27.7709544 | 191     | 53.1308698 | -27.8299421 | 192     | 53.1310120 | -27.8236125 |
| 193     | 53.1315421 | -27.7864976 | 194     | 53.1316813 | -27.8345866 | 195     | 53.1356372 | -27.7666907 |
| 196     | 53.1357641 | -27.8484238 | 197     | 53.1362945 | -27.7632657 | 198     | 53.1369272 | -27.7907591 |
| 199     | 53.1370804 | -27.8501197 | 200     | 53.1376604 | -27.7632512 | 201     | 53.1378387 | -27.8566923 |
| 202     | 53.1392775 | -27.7807792 | 203     | 53.1413527 | -27.8257550 | 204     | 53.1418679 | -27.8253231 |
| 205     | 53.1470842 | -27.7785246 | 206     | 53.1479323 | -27.7740950 | 207     | 53.1481753 | -27.7738463 |
| 208     | 53.1492580 | -27.7636845 | 209     | 53.1499215 | -27.8140455 | 210     | 53.1515470 | -27.8549017 |
| 211     | 53.1519920 | -27.7747388 | 212     | 53.1520962 | -27.8351648 | 213     | 53.1531176 | -27.8686182 |
| 214     | 53.1554066 | -27.7382866 | 215     | 53.1572340 | -27.7379451 | 216     | 53.1578600 | -27.7975775 |
| 217     | 53.1580437 | -27.8384650 | 218     | 53.1602537 | -27.7693798 | 219     | 53.1607121 | -27.7753929 |
| 220     | 53.1608299 | -27.7500577 | 221     | 53.1608511 | -27.7428529 | 222     | 53.1627502 | -27.7391179 |
| 223     | 53.1631045 | -27.8123967 | 224     | 53.1636135 | -27.8516310 | 225     | 53.1646982 | -27.8533656 |
| 226     | 53.1648402 | -27.7560441 | 227     | 53.1657665 | -27.8562203 | 228     | 53.1658978 | -27.7816064 |
| 229     | 53.1661972 | -27.7875825 | 230     | 53.1697386 | -27.8239961 | 231     | 53.1719913 | -27.8395618 |
| 232     | 53.1721962 | -27.7651716 | 233     | 53.1729385 | -27.7779153 | 234     | 53.1729692 | -27.7446003 |
| 235     | 53.1740883 | -27.7881150 | 236     | 53.1747265 | -27.8408071 | 237     | 53.1747682 | -27.7992826 |
| 238     | 53.1753216 | -27.7393471 | 239     | 53.1762360 | -27.7962420 | 240     | 53.1763802 | -27.8306977 |
| 241     | 53.1765762 | -27.7855088 | 242     | 53.1784236 | -27.7683139 | 243     | 53.1796778 | -27.7688462 |
| 244     | 53.1801045 | -27.7492538 | 245     | 53.1808938 | -27.7549298 | 246     | 53.1821319 | -27.7358393 |
| 247     | 53.1835660 | -27.7568481 | 248     | 53.1845989 | -27.7447883 | 249     | 53.1879459 | -27.7900924 |
| 250     | 53.1885059 | -27.7452762 | 251     | 53.1901361 | -27.7652570 | 252     | 53.1920889 | -27.7872543 |
| 253     | 53.1922054 | -27.7410196 | 254     | 53.2018256 | -27.7642261 | 255     | 53.2018992 | -27.7888604 |
| 256     | 53.2028329 | -27.7650603 | 257     | 53.2047339 | -27.7568440 | 258     | 53.2069528 | -27.7849266 |
| 259     | 53.2070046 | -27.7529810 | 260     | 53.2118685 | -27.7544650 | 261     | 53.2146651 | -27.7526799 |
| 262     | 53.2157378 | -27.7691409 | 263     | 53.2180201 | -27.7540485 |         |            |             |

#### 4 SUMMARY OF EXPERIMENTS SUGGESTING THAT THE DISTRIBUTION OF THE GALAXY DIRECTIONS OF ROTATION IS RANDOM

Section 1 mentions multiple studies using several different space- and Earth-based telescopes showing unequal distribution of the directions of rotation of galaxies (MacGillivray & Dodd 1985; Longo 2011; Shamir 2012, 2016, 2019, 2020b, c, d, 2021a, b, 2022a, b, d, e). Reports started as early as the 1980s (MacGillivray & Dodd 1985),

and include Earth-based telescopes such as Sloan Digital Sky Survey (SDSS) (Shamir 2019, 2020d, 2021a, 2022d), the Panoramic Survey Telescope and Rapid Response System (Pan-STARRS) (Shamir 2020d), the DES (Shamir 2022a), and DESI Legacy Survey (Shamir 2021b, 2022e), as well as space-based telescopes such as *HST* (Shamir 2020b) and *JWST* (Shamir 2024e).

Section 1 also mentions previous reports suggesting fully random distribution of the directions of rotations of galaxies. Although none



Downloaded from <https://academic.oup.com/mnras/article/538/1/76/8019798> by guest on 15 March 2025

**Figure 7.** Spiral galaxies imaged by *JWST* in the GOODS-S field of JADES that rotate in the same direction relative to the Milky Way (red), and in the opposite direction relative to the Milky Way (blue). The figure shows 158 galaxies that rotate in the opposite direction relative to the Milky Way, and just 105 that rotate in the same direction relative to the Milky Way. The analysed field covers the *JWST* GOODS-S JADES field imaged with the 4.4, 2.0, and 0.9  $\mu\text{m}$  bands.

of these studies used high redshifts space-based telescopes, these observations can be considered to be in conflict with the observation of unequal distribution shown in Section 3. Analyses of these experiments, including reproduction of the results, show that these experiments are in fact aligned with the non-random distribution as shown in Section 3. Explanations of these experiments as well as code and data to reproduce them can be found in Shamir (2023), and description of specific experiments can be found in Shamir (2022c, e) and Mcadam & Shamir (2023b).

One of the early experiments (Iye & Sugai 1991) tested the distribution by annotating the galaxies manually. Besides the limitations of

possible systematic biases of manual annotations, manual annotation is also highly limited by the volume of data that can be processed. The resulting data set only included 3257 galaxies rotating clockwise and 3268 galaxies rotating counterclockwise. As explained quantitatively in Shamir (2022c, e, 2023), Mcadam & Shamir (2023b), that data set was far too small to show a statistically significant difference for galaxies at relatively low redshift. Experiments using Earth-based telescopes used far larger data sets (Shamir 2022c, e, 2023; Mcadam & Shamir 2023b).

An experiment that received public attention was made by using anonymous volunteers to annotate the galaxies through the Internet

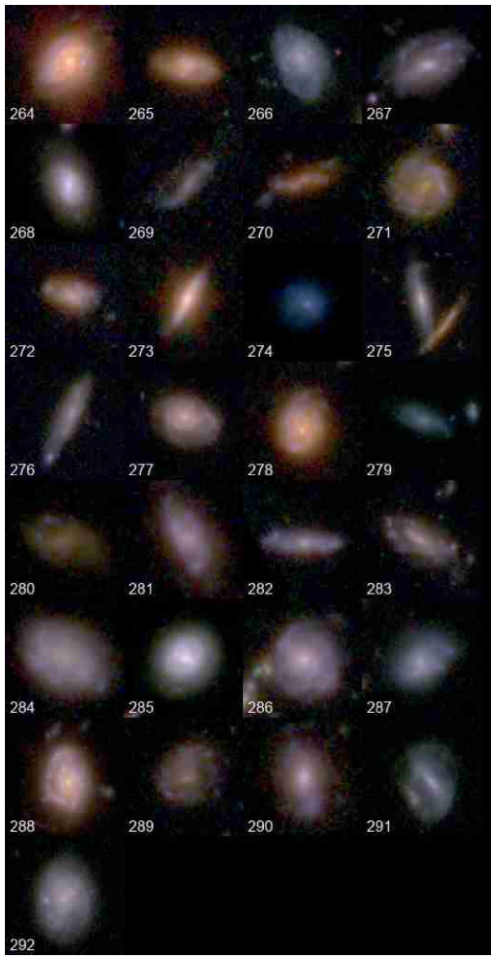


**Figure 8.** The galaxies in the JADES GOODS-S field that were not identified by the annotation algorithm, but were identified through manual inspection as galaxies that could be rotating in the same direction relative to the Milky Way (counterclockwise). The direction of rotation in these galaxies is not entirely clear from the images.

(Land et al. 2008). The use of a large number of human annotators provided a large number of annotations. The downside of the approach was that the annotations made by the volunteers had a substantial degree errors, making most annotated galaxies unusable due to the high level of disagreements between the annotators. More importantly, the human annotators had a bias towards galaxies that rotate counterclockwise, leading to an extreme bias of  $\sim 15$  per cent in the resulting ‘superclean’ data set. That bias did not allow to determine whether the excessive number of galaxies that rotate counterclockwise is driven by the Universe or by the bias of the volunteers who annotated them.

After the bias was noticed, a new experiment was done by annotating the original galaxy images as well as the mirrored images. But because the bias was noticed only after a very high number of galaxies were already annotated, the data set of the new experiment was relatively small, and included just  $\sim 1.1 \times 10^4$  annotated galaxies. The results are displayed in table 2 in Land et al. (2008). As also explained in Shamir (2022c, e, 2023, 2024e) and Mcadam & Shamir (2023b), the table shows a 1.5 per cent higher number of galaxies rotating counterclockwise in the first experiment, and 2.2 per cent in the second experiment. Due to the small number of galaxies the statistical significance was marginal, and becomes significant only

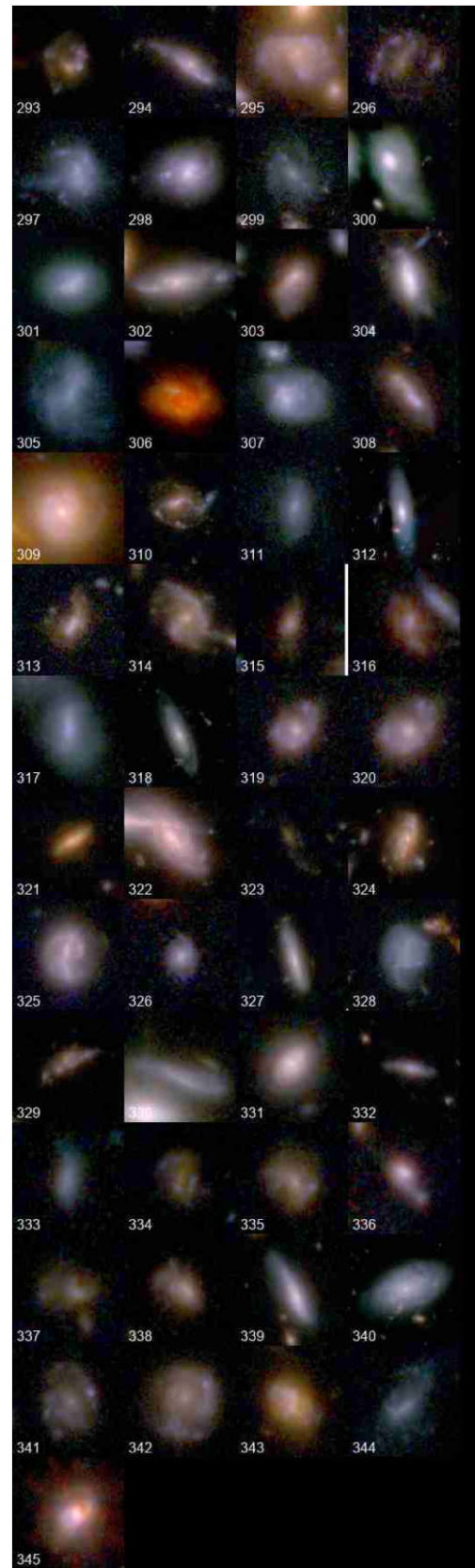


**Figure 9.** The galaxies in the JADES GOODS-S field that were not identified by the annotation algorithm, but were identified manually as galaxies that could be rotating in the opposite direction relative to the Milky Way.

**Table 3.** The RA and Dec. of the galaxies that rotate counterclockwise shown in Fig. 8.

| Numbers | RA         | Dec.        | Numbers | RA         | Dec.        | Numbers | RA         | Dec.        |
|---------|------------|-------------|---------|------------|-------------|---------|------------|-------------|
| 264     | 53.0384867 | -27.8622052 | 265     | 53.0502416 | -27.8402054 | 266     | 53.0571043 | -27.8209306 |
| 267     | 53.0734400 | -27.8408036 | 268     | 53.0784400 | -27.8194916 | 269     | 53.0938238 | -27.8941047 |
| 270     | 53.0960714 | -27.8286830 | 271     | 53.0968709 | -27.8855638 | 272     | 53.0979105 | -27.9080514 |
| 273     | 53.1119073 | -27.8053042 | 274     | 53.1205041 | -27.8517213 | 275     | 53.1315577 | -27.8963155 |
| 276     | 53.1329688 | -27.8984036 | 277     | 53.1393988 | -27.7674556 | 278     | 53.1411431 | -27.7618807 |
| 279     | 53.1435404 | -27.7557315 | 280     | 53.1500039 | -27.7577261 | 281     | 53.1523614 | -27.7780246 |
| 282     | 53.1588635 | -27.7574229 | 283     | 53.1607380 | -27.8358968 | 284     | 53.1644578 | -27.7659101 |
| 285     | 53.1673684 | -27.8405377 | 286     | 53.1675621 | -27.7925632 | 287     | 53.1807708 | -27.7568397 |
| 288     | 53.1812865 | -27.7656881 | 289     | 53.1821604 | -27.8058583 | 290     | 53.1898988 | -27.7413466 |
| 291     | 53.2070911 | -27.7641427 | 292     | 53.2093471 | -27.7609204 |         |            |             |

**Table 4.** The RA and Dec. of the galaxies that rotate clockwise shown in Fig. 9.

| Numbers | RA         | Dec.        | Numbers | RA         | Dec.        | Numbers | RA         | Dec.        |
|---------|------------|-------------|---------|------------|-------------|---------|------------|-------------|
| 293     | 53.0307616 | -27.8706095 | 294     | 53.0331686 | -27.8480343 | 295     | 53.0477066 | -27.8353006 |
| 296     | 53.0552493 | -27.8233445 | 297     | 53.0608612 | -27.8204453 | 298     | 53.0689281 | -27.8263187 |
| 299     | 53.0697976 | -27.8391838 | 300     | 53.0711214 | -27.8227704 | 301     | 53.0741950 | -27.8239991 |
| 302     | 53.0882270 | -27.8506168 | 303     | 53.0923399 | -27.8479983 | 304     | 53.0965038 | -27.9073124 |
| 305     | 53.1072662 | -27.8058498 | 306     | 53.1074781 | -27.8041212 | 307     | 53.1082963 | -27.8930911 |
| 308     | 53.1184803 | -27.8053588 | 309     | 53.1198685 | -27.7987721 | 310     | 53.1228467 | -27.8483623 |
| 311     | 53.1284391 | -27.8504606 | 312     | 53.1360779 | -27.8292005 | 313     | 53.1403351 | -27.8635211 |
| 314     | 53.1413943 | -27.8257229 | 315     | 53.1419006 | -27.8253096 | 316     | 53.1436493 | -27.7582272 |
| 317     | 53.1452409 | -27.7511319 | 318     | 53.1508174 | -27.7601240 | 319     | 53.1508706 | -27.8612319 |
| 320     | 53.1508807 | -27.8611853 | 321     | 53.1547878 | -27.7739138 | 322     | 53.1548761 | -27.8578577 |
| 323     | 53.1554620 | -27.8386084 | 324     | 53.1557427 | -27.7794153 | 325     | 53.1588282 | -27.7705852 |
| 326     | 53.1600134 | -27.8637361 | 327     | 53.1602644 | -27.8255784 | 328     | 53.1608377 | -27.8653308 |
| 329     | 53.1639085 | -27.7653675 | 330     | 53.1692446 | -27.7917806 | 331     | 53.1707031 | -27.7512668 |
| 332     | 53.1713223 | -27.7930262 | 333     | 53.1729254 | -27.7387797 | 334     | 53.1763369 | -27.8251897 |
| 335     | 53.1788946 | -27.7547901 | 336     | 53.1814716 | -27.8318782 | 337     | 53.1818135 | -27.8306672 |
| 338     | 53.1825614 | -27.8244443 | 339     | 53.1830999 | -27.7510514 | 340     | 53.1901582 | -27.7652015 |
| 341     | 53.1907319 | -27.7570106 | 342     | 53.1926134 | -27.7581417 | 343     | 53.2021859 | -27.7550068 |
| 344     | 53.2023063 | -27.7904402 | 345     | 53.2180747 | -27.7616774 |         |            |             |

when combining the two experiments (Shamir 2022c, 2023, 2024e; Mcadam & Shamir 2023b). But the asymmetry agrees on both the direction and the magnitude with the asymmetry shown in Shamir (2020d), which uses the same telescope and same footprint as the experiment of Land et al. (2008).

Hayes et al. (2017) used automation to annotate a large number of galaxies from the same telescope and footprint used in Land et al. (2008) and Shamir (2020d). The results are summarized in table 2 in Hayes et al. (2017), showing consistent results of an excessive number of galaxies that rotate counterclockwise. The experiment that provided random distribution was an experiment done by selecting the spiral galaxies by applying machine learning. Interestingly, the selection of the galaxies by using machine learning was done such that features that correlate with the direction of rotation of the galaxies were identified and removed manually. As stated in Hayes et al. (2017), ‘We choose our attributes to include some photometric attributes that were disjoint with those that Shamir (2016) found to be correlated with chirality, in addition to several SpArcFiRe outputs with all chirality information removed’. The discussion does not specify a reason for the decision to manually remove just these features.

After removing these features manually, the analysis provided random distribution. But that can also be expected because removing just the features that can identify galaxy direction of rotation would naturally weaken any signal of unequal number of galaxies that rotate in opposite direction. That is explained in detail in Mcadam

& Shamir (2023b), as well as in Shamir (2023). Reproduction of the experiment of Hayes et al. (2017) by using the exact same code and same data but without manually removing specific features showed a clear statistically significant asymmetry (Mcadam & Shamir 2023b), in good agreement with the asymmetry observed with SDSS and other telescopes. The full reproduction of the experiment with code and data is described in Mcadam & Shamir (2023b).

Another experiment used image data taken from the Hyper Suprime-Cam (HCS), and annotated it automatically using a deep neural network (Tadaki et al. 2020). That data analysis provided 38 718 galaxies that rotating clockwise and 37 917 galaxies rotating counterclockwise. Using simple binomial distribution, the one-tailed mere chance probability of the difference is  $p \simeq 0.0019$ . The higher number of galaxies that rotate clockwise agrees with the location of HCS footprint, which is closer to the Southern Galactic pole. As shown in Shamir (2022e) and in Fig. 10, a higher number of galaxies rotating clockwise is expected at around the Southern Galactic pole.

Since the deep neural network used for the annotation had a certain degree of error, and the error was higher than the asymmetry, the analysis was not considered statistically significant. But although the results cannot be considered a sound proof for the unequal distribution, they are in agreement with the other previous reports that show an unequal number of galaxies that rotate in opposite directions, and certainly do not conflict with them.

Jia, Zhu & Pen (2023) used deep neural networks to study the distribution of galaxy directions of rotation using data collected by

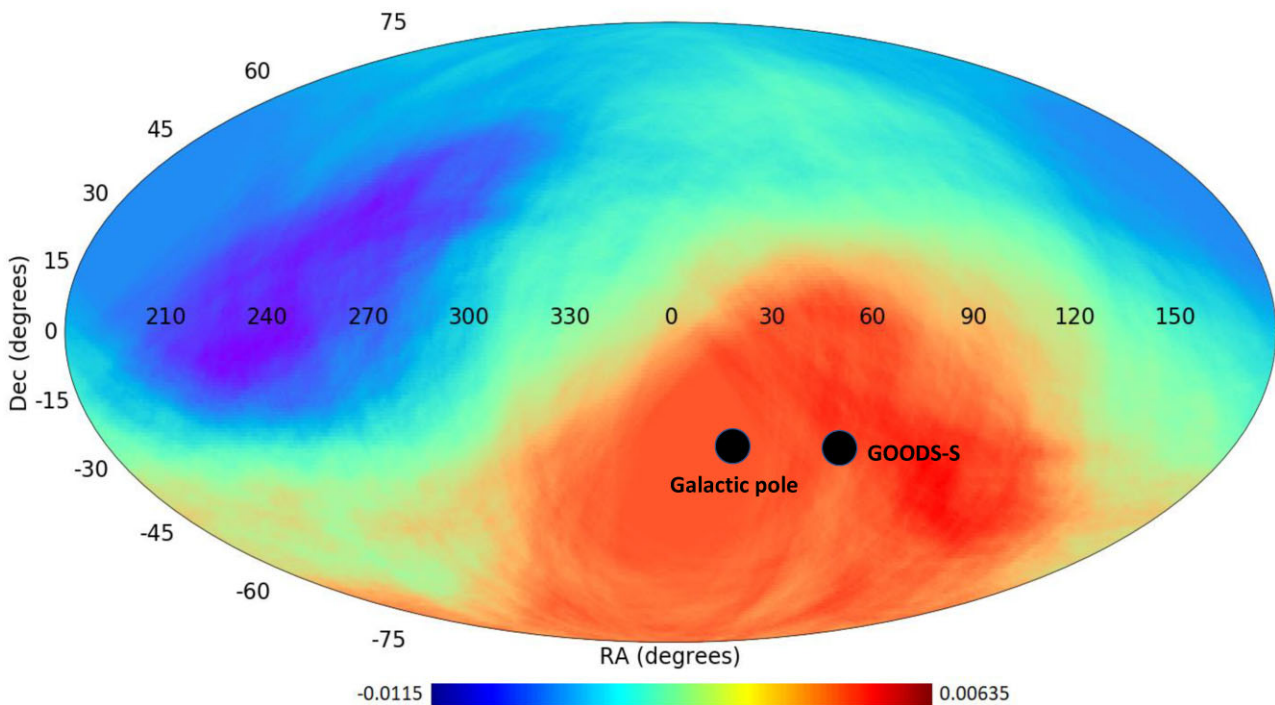


**Figure 10.** The differences in the number of galaxies with opposite directions of rotations in different parts of the sky as determined by using  $1.3 \times 10^6$  galaxies imaged by the DESI Legacy Survey (Shamir 2024e). The location of the GOODS-S field is at a part of the sky with a higher number of galaxies rotating clockwise.

SDSS and DESI. Due to the error in the annotation of the neural network, the experiment was done with different accuracy thresholds to balance between the accuracy of the annotations and the size of the data set. When increasing the accuracy threshold, the error in the annotation of the data decreases, but the size of the data set gets smaller since fewer galaxies meet the threshold.

The highest threshold used was 0.9, providing a data set of 9218 SDSS clockwise galaxies and 9442 counterclockwise SDSS galaxies, as shown in table 1 in Jia et al. (2023). The asymmetry of  $\sim 2.4$  per cent agrees with the asymmetry shown in Shamir (2020d), which is based on the same sky survey and therefore similar footprint. The one-tailed probability for the observation to occur by mere chance is  $\sim 0.05$ . That statistical significance is somewhat weaker than the statistical significance observed in Shamir (2020d), which can be expected due to the much higher number of galaxies used in Shamir (2020d). But although the  $p$  value is lower, it can still be considered statistically significant, and definitely not in conflict with the other observations as explained in Shamir (2024e).

The DESI Legacy Survey has a very large footprint that covers both hemispheres, and therefore it is difficult to predict the asymmetry as the asymmetry in one hemisphere is offset by the inverse asymmetry in the opposite hemispheres (Shamir 2024e). The analysis of Jia et al. (2023) found 11 649 clockwise galaxies and 11 919 counterclockwise galaxies. The probability of that asymmetry to occur by chance is 0.04. While the large footprint does not allow accurate analysis, the binomial distribution can be considered statistically significant, and does not conflict with the contention that the distribution of the directions of rotation of the galaxies is random.

Another experiment suggesting random distribution of galaxy directions of rotation claimed that the asymmetry shown in previous experiments is the result of ‘duplicate objects’ in the data set (Iye et al. 2021). This experiment is explained in detail and full reproduction

in Shamir (2022c, e, 2023). In summary, the catalogue used in Iye et al. (2021) was used in Shamir (2017b) for photometric analysis only, and no claim for a dipole axis formed by the distribution of the directions of rotation of galaxies was made based on that data set (Shamir 2022c, e, 2023).

More importantly, as shown in Shamir (2023), the reproduction of the experiment using the same data and same analysis method used in Iye et al. (2021) provides different results than the results shown in Iye et al. (2021), showing a statistically significant non-random distribution (Shamir 2023). Code and data that allows to easily reproduce the experiment are available at.<sup>1</sup> The link also provides the description of the reproduction of the National Astronomical Observatory of Japan (NAOJ) to explain the difference between the reproduction and the results shown in the paper. In summary, the NAOJ explains that ‘Because it is hard to verify the detail of simulations, we here calculate the analytic solution by Chandrasekhar (1943) which assumes uniform samples in the hemisphere’. But the assumption of a uniform sample is not correct for SDSS, which covers just a part of the hemisphere, and the density of the galaxy population varies substantially within its footprint. That assumption is not mentioned in Iye et al. (2021), and in fact is not needed since the exact locations of all galaxies are well known.

Another study (Patel & Desmond 2024) that suggested the distribution of the directions of rotation of galaxies is random was based on data used in previous studies (Longo 2011; Mcadam & Shamir 2023b). Instead of using the standard binomial distribution statistics and simple  $\chi^2$  statistics used in MacGillivray & Dodd (1985), Longo (2011), Shamir (2012, 2016, 2019, 2020b, c, d, 2021a, b, 2022a, b, d, e, 2023, 2024e), and Mcadam & Shamir

<sup>1</sup>[https://people.cs.ksu.edu/~lshamir/data/aye\\_et\\_al](https://people.cs.ksu.edu/~lshamir/data/aye_et_al)

(2023b), Patel & Desmond (2024) propose a new complex ad-hoc statistical method. The downside of the new method is that it does not respond to asymmetry in the distribution of galaxy spin directions (Shamir 2024a, d). As explained in Shamir (2024a), even in cases where synthetic asymmetry is added to the data to create a highly asymmetric data set, the method still reports random distribution.

For instance, Patel & Desmond (2024) applied the new method to the data set used in Mcadam & Shamir (2023b), annotated as ‘GAN M’ in Patel & Desmond (2024). It is publicly available at <https://people.cs.ksu.edu/~lshamir/data/sparcfire/>. The data set was annotated by the *SpArcFiRe* algorithm for the purpose of reproducing the results shown in Hayes et al. (2017), not necessarily to study the Universe due to the known bias in the annotation method. As noted in the appendix of Hayes et al. (2017), *SpArcFiRe* has a known bias, and therefore a dataset annotated by it is expected to show a difference between the number of galaxies rotating clockwise and the number of galaxies rotating counterclockwise. Indeed, the data set of 139 852 galaxies annotated by *SpArcFiRe* is separated to 70 672 counterclockwise galaxies and 69 180 clockwise galaxies. Using standard binomial statistics, the two-tailed probability to have such asymmetry by chance is  $\sim 0.00006$ . But as reported in the fourth row of table 4 in Patel & Desmond (2024), the new statistical method provided a non-significant *p*-value of 0.25. The fact that applying the new method to an extremely asymmetric synthetic data shows a null-hypothesis universe with no statistically significant asymmetry, indicating that the new method does not guarantee to identify asymmetry (Patel & Desmond 2024).

Patel & Desmond (2024) also argued that the reproduction of previous results of Longo (2011) and Mcadam & Shamir (2023b) provided different results than the results stated in these papers, as stated in section 4.3 in Patel & Desmond (2024). That claim has also shown to be incorrect, with code and step-by-step instructions to easily reproduce the results of both papers. The full open code and step-by-step instructions can be found at [https://people.cs.ksu.edu/~lshamir/data/patel\\_desmond/](https://people.cs.ksu.edu/~lshamir/data/patel_desmond/).

## 5 CONCLUSION

*JWST* has provided unprecedented imaging power that allows to observe high visual details of galaxies in the deep Universe. Despite being relatively new, observations made in *JWST* deep fields have already challenged some of the foundational assumptions regarding the Universe. Here, *JWST* shows that the number of galaxies that rotate in the opposite direction relative to the Milky Way as observed from Earth is higher than the number of galaxies that rotate in the same direction relative to the Milky Way. The observation was made also with initial *JWST* data (Shamir 2024e), and was also noticed in the UDF imaged by *HST* (Shamir 2021c), but JADES allows to observe the asymmetry in the early Universe using a much higher number of galaxies. The analysis is done by a defined quantitative criteria, but the asymmetry is high and can be inspected also by the unaided human eye.

As discussed in Introduction, the asymmetry between galaxies that rotate in opposite directions was noticed in numerous studies starting the 1980s, and more recent experiments include analysis of very large data sets collected by autonomous digital sky surveys. The magnitude of the asymmetry observed through *JWST* is stronger than the magnitude of the asymmetry reported previously using Earth-based data. That can be linked to the previous observation that the magnitude of the asymmetry increases as the redshift gets higher (Shamir 2019, 2020d, 2022d, 2024d). For instance, table 5, taken from Shamir (2020d), shows the distribution of spiral galaxies

**Table 5.** The distribution of galaxies rotating clockwise and counterclockwise imaged by SDSS. All galaxies are within the RA range of  $(120^\circ, 210^\circ)$ . The *p*-values are the binomial distribution *p*-value to have such asymmetry or stronger by chance. The table is taken from Shamir (2020d).

| <i>z</i> | cw     | ccw    | $\frac{\text{cw}}{\text{cw}+\text{ccw}}$ | <i>p</i> -value       |
|----------|--------|--------|--|-----------------------|
| 0–0.05   | 3216   | 3180   | 0.5003                                   | 0.698                 |
| 0.05–0.1 | 6240   | 6270   | 0.498                                    | 0.4                   |
| 0.1–0.15 | 4236   | 4273   | 0.496                                    | 0.285                 |
| 0.15–0.2 | 1586   | 1716   | 0.479                                    | 0.008                 |
| 0.2–0.5  | 2598   | 2952   | 0.469                                    | $1.07 \times 10^{-6}$ |
| Total    | 17 876 | 18 391 | 0.493                                    | 0.0034                |

imaged by SDSS at different redshift ranges. The RA is limited to  $(120^\circ, 210^\circ)$ , which is around the location of the Northern end of the Galactic pole.

As the table shows, the asymmetry increases as the redshift gets higher. While there is no proven link between the observation made with *JWST* and the information provided in Table 5, it should remain a possibility that the observations are linked. In that case, the asymmetry changes gradually with time or distance from Earth.

Possible explanations to the observation can be broadly divided into two categories: the first is an anomaly in the large-scale structure (LSS) of the early universe, and the second is related to the physics of galaxy rotation.

### 5.1 Anomaly in the LSS

If the observation shown here indeed reflects the structure of the Universe, it shows that the early universe was more homogeneous in terms of the directions towards which galaxies rotate, and becomes more chaotic over time while exhibiting a cosmological-scale axis that is close to the Galactic pole. Some cosmological models assume a geometry that features a cosmological-scale axis. These include ellipsoidal Universe (Campanelli, Cea & Tedesco 2006, 2007; Gruppuso 2007; Campanelli et al. 2011; Cea 2014), dipole big bang (Allahyari et al. 2025; Krishnan, Mondol & Sheikh-Jabbari 2023), and isotropic inflation (Feng & Zhang 2003; Piao, Feng & Zhang 2004; Bohmer & Mota 2008; Edelstein, Rodríguez & López 2020; Arciniega et al. 2020a; Arciniega, Edelstein & Jaime 2020b; Jaime 2021; Dainotti et al. 2022; Luongo et al. 2022). In these cases, the large-scale distribution of the galaxy rotation is aligned in the form of a cosmological-scale axis, and the location of that axis in close proximity to the Galactic pole can be considered a coincidence.

An additional cosmological model that requires the assumption of a cosmological-scale axis is the theory of rotating Universe (Gödel 1949; Ozsváth & Schücking 1962; Ozsvath & Schücking 2001; Sivaram & Arun 2012; Chechin 2016; Campanelli 2021; Seshavatharam & Lakshminarayana 2021). That model is also related to the theory of black hole cosmology (Pathria 1972; Stuckey 1994; Easson & Brandenberger 2001; Tatum et al. 2018; Chakrabarty et al. 2020), according which the Universe is the interior of black hole in a parent universe, and therefore is also aligned with the contention of multiverse.

Because black holes spin (McClintock et al. 2006; Mudambi et al. 2020; Reynolds 2021), a universe hosted inside of a black hole is also expected to spin. Therefore, it has been proposed that a universe located in the interior of a black hole should have an axis, and inherit the preferred direction of the host black hole (Popławski 2010; Seshavatharam 2010; Christillin 2014; Seshavatharam &

Lakshminarayana 2020, 2021). Black hole cosmology is also linked to the theory of holographic universe (Susskind 1995; Bak & Rey 2000; Bouso 2002; Myung 2005; Hu & Ling 2006; Sivaram & Arun 2013; Shor, Benninger & Khrennikov 2021; Rinaldi et al. 2022).

Another paradigm relevant to the observation described here is the contention that the LSS of the Universe has a fractal structure, reflected by fractal patterns formed by the large-scale distribution galaxies (Baryshev et al. 1998; Baryshev 2000; Pietronero & Labini 2000; Labini & Pietronero 2001; Labini & Gabrielli 2003, 2004; Gabrielli et al. 2005; Teles, Lopes & Ribeiro 2022). These patterns challenge the assumption that the distribution of galaxies in the LSS is random.

These explanations are considered alternative to the standard cosmological model (Turner 1996; Pecker 1997; Perivolaropoulos 2014; Bull et al. 2016; Netchitailo et al. 2020; Velten & Gomes 2020), and also violates the isotropy assumption of the Cosmological Principle. Although the Cosmological Principle is the basic assumption for the standard cosmological model, its correctness has been challenged (Pecker 1997; Kroupa 2012). Observations using a variety of different probes have also challenged the correctness of the Cosmological Principle in an empirical manner (Aluri et al. 2023).

## 5.2 Physics of galaxy rotation

As mentioned above, if the distribution of directions of rotation of galaxies indeed form a cosmological-scale axis, the alignment of that axis with the Galactic pole could be considered a coincidence. But another explanation could be that the distribution of galaxy direction of rotation in the Universe is random, but only seems non-random to an Earth-based observer. In that case, the observation can be explained by the effect of the rotational velocity of the observed galaxies relative to the rotational velocity of Earth around the centre of the Milky Way galaxy. That can explain the observation without violating the Cosmological Principle. The proximity to the Galactic pole is expected, as the difference between the rotational velocity of the Milky Way and the rotational velocity of the observed galaxies peaks at the Galactic pole.

As discussed in Shamir (2017a, 2020a) and McAdam & Shamir (2023a), due to the Doppler shift effect galaxies that rotate in the opposite direction relative to the Milky Way are expected to be slightly brighter than galaxies that rotate in the same direction relative to the Milky Way. Therefore, more galaxies that rotate in the opposite direction relative to the Milky Way are expected to be observed from Earth, and the difference should peak at around the Galactic pole. That observation is conceptually aligned with the empirical data of Fig. 10, and the observation using JADES described in Section 3.

This explanation is challenged by the fact that the effect of the rotational velocity have merely a mild impact on the brightness of galaxies, and therefore is not expected to lead to the dramatic difference of  $\sim 50$  per cent in the number of galaxies as observed through JADES. On the other hand, empirical observations showed that the difference in brightness is larger than expected given the rotational velocity of galaxies (Shamir 2017a, 2020a; McAdam & Shamir 2023a). That was observed with SDSS (McAdam & Shamir 2023a), Pan-STARRS (Shamir 2017a), and the space-based *HST* (Shamir 2020a). Similar observations were made with the redshift (Shamir 2024b, c), also showing that the magnitude of the asymmetry increases as the redshift gets larger (Shamir 2024b). Other related observations can be the dipole formed by quasar distribution as observed from Earth (Hutsemékers et al. 2014; Secret et al. 2021), which has been shown to be linked to the colour (Panwar, Jain &

Omar 2024), and therefore could also be a photometric effect rather than a feature of the LSS of the Universe. The number of galaxies in the line of sight also show a surprising cosmological-scale anisotropy (Ahn 2025), and that can also be related to the differences in the brightness of galaxies as observed from Earth.

The difference can be linked to the mysterious physics of galaxy rotation, which is known to be in substantial tension with the mass (Oort 1940; Rubin 1983). Common explanations include dark matter (Rubin 1983; El-Neaj et al. 2020), modified Newtonian dynamics (Milgrom 1983), and others (Sanders 1990; Capozziello & De Laurentis 2012; Chadwick, Hodgkinson & McDonald 2013; Farnes 2018; Nagao 2020; Rivera 2020; Blake 2021; Gomel & Zimmerman 2021; Skordis & Złotnicki 2021; Larin 2022), but no explanation has been fully proven. In particular, the theory of dark matter as the explanation to the difference between the mass and rotational velocity of stars within galaxies has been challenged, and despite over a century of research there is still no clear proven explanation to the physics of galaxy rotation (Sanders 1990; Mannheim 2006; Kroupa 2012, 2015; Kroupa, Pawłowski & Milgrom 2012; Akerib et al. 2017; Arun, Gudennavar & Sivaram 2017; Aprile et al. 2018; Bertone & Tait 2018; Skordis & Złotnicki 2019; Hofmeister & Criss 2020; Sivaram, Arun & Rebecca 2020; Byrd & Howard 2021). Therefore, it is possible that the physics of galaxy rotation, which is not yet fully known, affects the brightness of the galaxy in a manner that is not necessarily expected.

If the physics of galaxy rotation affects the light that galaxies emit in a manner that is currently unknown, that can also affect the redshift, and therefore can be related to alternative redshift models (Crawford 1999; Shao 2013; Kragh 2017; Shao, Wang & Gao 2018; Sato 2019; LaViolette 2021; Lovyagin et al. 2022; Fulton 2023; Lee 2023; Lopez-Corredoira 2023; Pletcher 2023; Seshavatharam & Lakshminarayana 2023; Gupta 2024a). Although the physical mechanism of such phenomenon is not clear, using alternative redshift models can explain a large number of observations that are currently unexplained such as dark energy, the  $H_0$  tension (Wu & Huterer 2017; Bolejko 2018; Mörtsell & Dhawan 2018; Davis et al. 2019; Camarena & Marra 2020; Pandey et al. 2020; Di Valentino et al. 2021; Riess et al. 2022), as well as the unexpected presence of large and massive galaxies in the early Universe (Xiao et al. 2024; Glazebrook et al. 2024) that challenge the age of the Universe as estimated by the existing models. The age of the Universe has been challenged also by the presence of stars that are older than the estimated age of the Universe such as HD 140283 (Guillaume et al. 2024). These tensions challenge modern cosmology, and trigger a variety of solutions and explanations that involve new physics. These puzzling observations can be solved by using an alternative the redshift model (Crawford 1999; Shao 2013, 2019; Kragh 2017; Shao et al. 2018; LaViolette 2021; Lovyagin et al. 2022; Fulton 2023; Gupta 2023, 2024a; Lee 2023; Lopez-Corredoira 2023; Pletcher 2023; Seshavatharam & Lakshminarayana 2023). Although the physics that can lead to alternative redshift models is also not yet known, it can explain the observed tensions regarding the expansion rate and age of the Universe.

The unprecedented power of *JWST*, combined with other recent observations have revolutionized cosmology, and triggered substantial changes in the studying of the Universe. It is likely that research efforts to explain them will continue in the next few decades. The observation reported here can provide yet another piece of information that can ultimately lead to a complete model that can provide a consolidated explanation to all current unexplained observations.

## ACKNOWLEDGEMENTS

I would like to thank the knowledgeable reviewer and associate editor for the insightful comments. The study was supported in part by National Science Foundation grant 2148878.

## DATA AVAILABILITY

The data used in this study are available in the tables included in the manuscript. URLs to relevant data sets from previous papers are also provided in the body of the manuscript.

## REFERENCES

Adams N. et al., 2023, *MNRAS*, 518, 4755  
 Adil S. A., Mukhopadhyay U., Sen A. A., Vagnozzi S., 2023, *J. Cosmol. Astropart. Phys.*, 2023, 072  
 Ahn K., 2025, *J. Korean Phys. Soc.*, 86, 145  
 Akerib D. S. et al., 2017, *Phys. Rev. Lett.*, 118, 021303  
 Allahyari A., Ebrahimian E., Mondol R., Sheikh-Jabbari M., 2025, *Eur. Phys. J. C.*, 85, 119  
 Aluri P. K. et al., 2023, *Class. Quantum Gravity*, 40, 094001  
 Aprile E. et al., 2018, *Phys. Rev. Lett.*, 121, 111302  
 Arciniega G., Bueno P., Cano P. A., Edelstein J. D., Hennigar R. A., Jaime L. G., 2020a, *Phys. Lett. B*, 802, 135242  
 Arciniega G., Edelstein J. D., Jaime L. G., 2020b, *Phys. Lett. B*, 802, 135272  
 Arun K., Gudennavar S., Sivaram C., 2017, *Adv. Space Res.*, 60, 166  
 Bak D., Rey S.-J., 2000, *Class. Quantum Gravity*, 17, L1  
 Ball P., 2023, *Nature*, 624, 22  
 Baryshev Y. V., 2000, *Astron. Astrophys. Trans.*, 19, 417  
 Baryshev Y. V., Labini F. S., Montuori M., Pietronero L., Teerikorpi P., 1998, *Fractals*, 06, 231  
 Bertone G., Tait T. M., 2018, *Nature*, 562, 51  
 Blake B. C., 2021, *Bull. Am. Phys. Soc.*, 2021, B17.00002  
 Bohmer C. G., Mota D. F., 2008, *Phys. Lett. B*, 663, 168  
 Bolejko K., 2018, *Phys. Rev. D*, 97, 103529  
 Bousso R., 2002, *Rev. Mod. Phys.*, 74, 825  
 Boylan-Kolchin M., 2023, *Nat. Astron.*, 7, 731  
 Bradley L. D. et al., 2023, *ApJ*, 955, 13  
 Bull P. et al., 2016, *Phys. Dark Universe*, 12, 56  
 Bunker A. J. et al., 2024, *A&A*, 690, A288  
 Byrd G., Howard S., 2019, *J. Wash. Acad. Sci.*, 105, 1  
 Byrd G., Howard S., 2021, *J. Wash. Acad. Sci.*, 107, 1  
 Camarena D., Marra V., 2020, *Phys. Rev. Res.*, 2, 013028  
 Campanelli L., 2021, *Found. Phys.*, 51, 56  
 Campanelli L., Cea P., Fogli G., Tedesco L., 2011, *Mod. Phys. Lett. A*, 26, 1169  
 Campanelli L., Cea P., Tedesco L., 2006, *Pjys. Rev. Lett.*, 97, 131302  
 Campanelli L., Cea P., Tedesco L., 2007, *Phys. Rev. D*, 76, 063007  
 Capozziello S., De Laurentis M., 2012, *Ann. Phys.*, 524, 545  
 Carniani S. et al., 2024, *Nature*, 633, 318  
 Cea P., 2014, *MNRAS*, 441, 1646  
 Chadwick E. A., Hodgkinson T. F., McDonald G. S., 2013, *Phys. Rev. D*, 88, 024036  
 Chakrabarty H., Abdujabbarov A., Malafarina D., Bambi C., 2020, *Eur. Phys. J. C*, 80, 1  
 Chechin L., 2016, *Astron. Rep.*, 60, 535  
 Christillin P., 2014, *Eur. Phys. J. Plus*, 129, 1  
 Costantin L. et al., 2023, *Nature*, 623, 499  
 Crawford D. F., 1999, *Aust. J. Phys.*, 52, 753  
 Dainotti M. G., De Simone B., Schiavone T., Montani G., Rinaldi E., Lambiase G., Bogdan M., Ugale S., 2022, *Galaxies*, 10, 24  
 Davis T. M., Hinton S. R., Howlett C., Calcino J., 2019, *MNRAS*, 490, 2948  
 De Vaucouleurs G., 1958, *ApJ*, 127, 487  
 Dhar S., Shamir L., 2021, *Visual Inform.*, 5, 92  
 Dhar S., Shamir L., 2022, *A&C*, 38, 100545  
 Di Valentino E. et al., 2021, *Class. Quantum Gravity*, 38, 153001  
 Dolgov A., 2023, preprint ([arXiv:2310.00671](https://arxiv.org/abs/2310.00671))  
 Easson D. A., Brandenberger R. H., 2001, *J. High Energy Phys.*, 2001, 024  
 Edelstein J. D., Rodríguez D. V., López A. V., 2020, *J. Cosmol. Astropart. Phys.*, 2020, 040  
 Eisenstein D. J. et al., 2023, preprint ([arXiv:2306.02465](https://arxiv.org/abs/2306.02465))  
 El-Neaj Y. A. et al., 2020, *EPJ Quant. Technol.*, 7, 1  
 Erukude S. T., Joshi A., Shamir L., 2024, *Computers*, 13, 341  
 Farnes J. S., 2018, *A&A*, 620, A92  
 Feng B., Zhang X., 2003, *Phys. Lett. B*, 570, 145  
 Forconi M., Melchiorri A., Mena O., Menci N., et al., 2023, *J. Cosmol. Astropart. Phys.*, 2023, 012  
 Freeman T., Byrd G., Howard S., 1991, *BASS*, 23, 1460  
 Fulton D., 2023, *Cosmological Redshift via Non-Linear Frequency Down-Conversion of Electromagnetic Radiation*.  
 Gabrielli A., Labini F. S., Joyce M., Pietronero L., 2005, *Statistical Physics for Cosmic Structures*. Springer-Verlag, Berlin, p. 101  
 Glazebrook K. et al., 2024, *Nature*, 628, 277  
 Gödel K., 1949, *Rev. Mod. Phys.*, 21, 447  
 Gomel R., Zimmerman T., 2021, *Galaxies*, 9, 34  
 Gruppuso A., 2007, *Phys. Rev. D*, 76, 083010  
 Guillaume C., Buldgen G., Amarsi A., Dupret M., Lundkvist M., Larsen J., Scuflaire R., Noels A., 2024, *A&A*, 692, L3  
 Gupta R. P., 2023, *MNRAS*, 524, 3385  
 Gupta R. P., 2024b, *Universe*, 10, 266  
 Gupta R., 2024a, *ApJ*, 964, 55  
 Hayes W. B., Davis D., Silva P., 2017, *MNRAS*, 466, 3928  
 Helton J. M. et al., 2024, preprint ([arXiv:2405.18462](https://arxiv.org/abs/2405.18462))  
 Hofmeister A. M., Criss R. E., 2020, *Galaxies*, 8, 54  
 Hu B., Ling Y., 2006, *Phys. Rev. D*, 73, 123510  
 Hutsemékers D., Braibant L., Pelgrims V., Sluse D., 2014, *A&A*, 572, A18  
 Iye M., Sugai H., 1991, *ApJ*, 374, 112  
 Iye M., Tadaki K., Fukumoto H., 2019, *ApJ*, 886, 133  
 Iye M., Yagi M., Fukumoto H., 2021, *ApJ*, 907, 123  
 Jaime L. G., 2021, *Phys. Dark Universe*, 34, 100887  
 Jain R., Wadadekar Y., 2024, preprint ([arXiv:2412.04834](https://arxiv.org/abs/2412.04834))  
 Jia H., Zhu H.-M., Pen U.-L., 2023, *ApJ*, 943, 32  
 Jones G. C. et al., 2025, *MNRAS*, 536, 2355  
 Kragh H., 2017, *J. Astron. Hist. Her.*, 20, 2  
 Krishnan C., Mondol R., Sheikh-Jabbari M., 2023, *J. Cosmol. Astropart. Phys.*, 2023, 020  
 Kroupa P., 2012, *Publ. Astron. Soc. Aust.*, 29, 395  
 Kroupa P., 2015, *Can. J. Phys.*, 93, 169  
 Kroupa P., Pawłowski M., Milgrom M., 2012, *Int. J. Mod. Phys. D*, 21, 1230003  
 Kuhn V., Guo Y., Martin A., Bayless J., Gates E., Puleo A., 2024, *ApJ*, 968, L15  
 Labini F. S., Gabrielli A., 2003, *Institute of Physics Conference Series*. Institute of Physics, Philadelphia, p. 305  
 Labini F. S., Gabrielli A., 2004, *Phys. A: Stat. Mech. Appl.*, 338, 44  
 Labini F. S., Pietronero L., 2001, *Phase Transitions in the Early Universe: Theory and Observations*. Springer, Dordrecht  
 Land K. et al., 2008, *MNRAS*, 388, 1686  
 Larin S. A., 2022, *Universe*, 8, 632  
 LaViolette P. A., 2021, *Int. J. Astron. Astrophys.*, 11, 190  
 Lee S., 2023, *Phys. Dark Universe*, 42, 101286  
 Longo M. J., 2011, *Phys. Lett. B*, 699, 224  
 Lopez-Corredoira M., 2023, preprint ([arXiv:2307.10606](https://arxiv.org/abs/2307.10606))  
 Lovell C. C., Harrison I., Harikane Y., Tacchella S., Wilkins S. M., 2023, *MNRAS*, 518, 2511  
 Lovyagin N., Raikov A., Yershov V., Lovyagin Y., 2022, *Galaxies*, 10, 108  
 Luongo O., Muccino M., Colgáin E. Ó., Sheikh-Jabbari M., Yin L., 2022, *Phys. Rev. D*, 105, 103510  
 MacGillivray H., Dodd R., 1985, *A&A*, 145, 269  
 Mannheim P. D., 2006, *Prog. Part. Nucl. Phys.*, 56, 340  
 McAdam D., Shamir L., 2023a, *Symmetry*, 15, 1190  
 McAdam D., Shamir L., 2023b, *Adv. Astron.*, 2023, 1  
 McClintock J. E., Shafee R., Narayan R., Remillard R. A., Davis S. W., Li L.-X., 2006, *ApJ*, 652, 518

Melia F., 2023, *MNRAS*, 521, L85

Milgrom M., 1983, *AJ*, 270, 365

Morháč M., Kliman J., Matoušek V., Veselský M., Turzo I., 2000, *Nucl. Instrum. Methods Phys. Res. A*, 443, 108

Mörtsell E., Dhawan S., 2018, *J. Cosmol. Astropart. Phys.*, 2018, 025

Mudambi S. P., Rao A., Gudennavar S., Misra R., Bubbly S., 2020, *MNRAS*, 498, 4404

Muñoz J. B., Mirocha J., Chisholm J., Furlanetto S. R., Mason C., 2024, *MNRAS*, 535, L37

Myung Y. S., 2005, *Phys. Lett. B*, 610, 18

Nagao S., 2020, *Rep. Adv. Phys. Sci.*, 04, 2050004

Netchitailo V. S. et al., 2020, *J. High Energy Phys. Gravit. Cosmol.*, 06, 133

Oort J. H., 1940, *AJ*, 91, 273

Ozsváth I., Schücking E., 1962, *Nature*, 193, 1168

Ozsvath I., Schücking E., 2001, *Class. Quantum Gravity*, 18, 2243

Pandey S., Raveri M., Jain B., 2020, *Phys. Rev. D*, 102, 023505

Panwar M., Jain P., Omar A., 2024, *MNRAS*, 535, L63

Patel D., Desmond H., 2024, *MNRAS*, 534, 1553

Pathria R., 1972, *Nature*, 240, 298

Pecker J.-C., 1997, *JA&A*, 18, 323

Perivolaropoulos L., 2014, *Galaxies*, 2, 22

Piao Y.-S., Feng B., Zhang X., 2004, *Phys. Rev. D*, 69, 103520

Pietronero L., Labini F. S., 2000, *Phys. A: Stat. Mech. Appl.*, 280, 125

Pletcher A. E., 2023, *Qeios*, 10.32388/2X1GDL.2

Popławski N. J., 2010, *Phys. Lett. B*, 694, 181

Reynolds C. S., 2021, *ARA&A*, 59, 117

Riess A. G. et al., 2022, *ApJ*, 934, L7

Rinaldi E., Han X., Hassan M., Feng Y., Nori F., McGuigan M., Hanada M., 2022, *Phys. Rev. X Quant.*, 3, 010324

Rivera P. C., 2020, *Am. J. Astron. Astrophys.*, 7, 73

Rubin V. C., 1983, *Science*, 220, 1339

Sanders R., 1990, *A&AR*, 2, 1

Sato M., 2019, *Phys. Essays*, 32, 43

Schouws S. et al., 2024, preprint ([arXiv:2409.20549](https://arxiv.org/abs/2409.20549))

Secrest N., Hausegger S., Rameez M., Mohayee R., Sarkar S., Colin J., 2021, *ApJ*, 908, L51

Seshavatharam U. S., Lakshminarayana S., 2023, *Phys. Sci. Forum.*, 7, 43

Seshavatharam U., 2010, *Prog. Phys.*, 2, 7

Seshavatharam U., Lakshminarayana S., 2020, *Int. Astron. Astrophys. Res.*, 10, 247

Seshavatharam U., Lakshminarayana S., 2021, *Int. Astron. Astrophys. Res.*, 2, 282

Shamir L., 2011a, Astrophysics Source Code Library, record ascl:1105.011

Shamir L., 2011b, *ApJ*, 736, 141

Shamir L., 2012, *Phys. Lett. B*, 715, 25

Shamir L., 2013, *Galaxies*, 1, 210

Shamir L., 2016, *ApJ*, 823, 32

Shamir L., 2017a, *Publ. Astron. Soc. Aust.*, 34, e44

Shamir L., 2017b, *Publ. Astron. Soc. Aust.*, 34, e011

Shamir L., 2017c, *Ap&SS*, 362, 33

Shamir L., 2019, Large-scale patterns of galaxy spin rotation show cosmological-scale parity violation and multipoles, preprint ([arXiv:1912.05429](https://arxiv.org/abs/1912.05429))

Shamir L., 2020a, *Open Astron.*, 29, 15

Shamir L., 2020b, *Publ. Astron. Soc. Aust.*, 37, e053

Shamir L., 2020c, *Astron. Nachr.*, 341, 324

Shamir L., 2020d, *Ap&SS*, 365, 136

Shamir L., 2021a, *Particles*, 4, 11

Shamir L., 2021b, *Publ. Astron. Soc. Aust.*, 38, e037

Shamir L., 2021c, AAS Meeting, 230, 8

Shamir L., 2022a, *Universe*, 8, 397

Shamir L., 2022b, *JA&A*, 43, 24

Shamir L., 2022c, *PASJ*, 74, 1114

Shamir L., 2022d, *Astron. Nachr.*, 343, e20220010

Shamir L., 2022e, *MNRAS*, 516, 2281

Shamir L., 2023, *Symmetry*, 15, 9

Shamir L., 2024a, preprint ([arXiv:2404.13864](https://arxiv.org/abs/2404.13864))

Shamir L., 2024b, *Particles*, 7, 703

Shamir L., 2024c, *Universe*, 10, 129

Shamir L., 2024d, *Symmetry*, 16, 1389

Shamir L., 2024e, *Publ. Astron. Soc. Aust.*, 41, e038

Shao M.-H., 2013, *Phys. Essays*, 26, 183

Shao M.-H., Wang N., Gao Z.-F., 2018, Redefining Standard Model Cosmology. IntechOpen, London, p. 13

Shen X., Vogelsberger M., Boylan-Kolchin M., Tacchella S., Naidu R. P., 2024, *MNRAS*, 533, 3923

Shor O., Benninger F., Khrennikov A., 2021, *Entropy*, 23, 584

Sivaram C., Arun K., 2012, *Open Astron.*, 5, 7

Sivaram C., Arun K., 2013, *Ap&SS*, 348, 217

Sivaram C., Arun K., Rebecca L., 2020, *JA&A*, 41, 1

Skordis C., Złoński T., 2019, *Phys. Rev. D*, 100, 104013

Skordis C., Złoński T., 2021, *Phys. Rev. Lett.*, 127, 161302

Stuckey W., 1994, *Am. J. Phys.*, 62, 788

Susskind L., 1995, *J. Math. Phys.*, 36, 6377

Tadaki K.-i., Iye M., Fukumoto H., Hayashi M., Rusu C. E., Shimakawa R., Tosaki T., 2020, *MNRAS*, 496, 4276

Tatum E. T., et al., 2018, *J. Mod. Phys.*, 09, 1867

Teles S., Lopes A. R., Ribeiro M. B., 2022, *Eur. Phys. J. C*, 82, 896

Tsukui T., Iguchi S., 2021, *Science*, 372, 1201

Turner M. S., 1996, *Phys. World*, 9, 31

Velten H., Gomes S., 2020, *Phys. Rev. D*, 101, 043502

Wang D., Liu Y., 2023, preprint ([arXiv:2301.00347](https://arxiv.org/abs/2301.00347))

Wu H.-Y., Huterer D., 2017, *MNRAS*, 471, 4946

Xiao M. et al., 2024, *Nature*, 635, 311

This paper has been typeset from a *TeX/LaTeX* file prepared by the author.